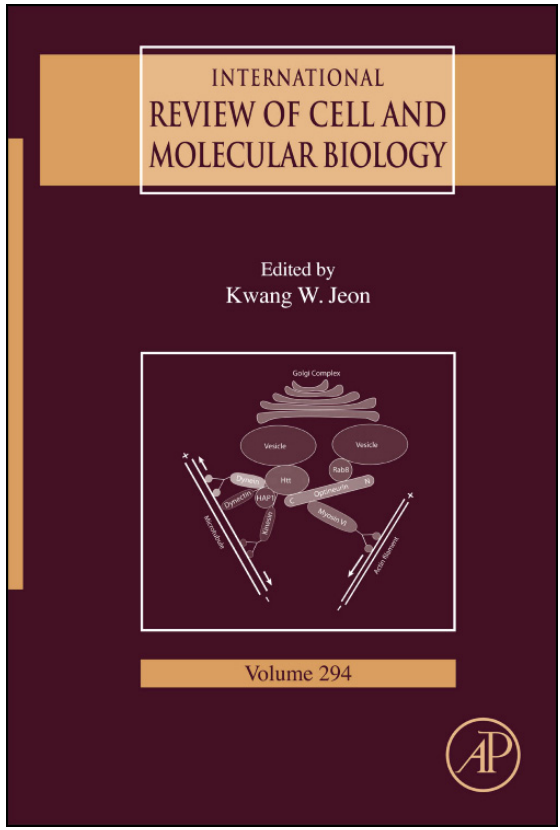

From: Wolfgang B. Fischer, Yi-Ting Wang, Christina Schindler, and Chin-Pei Chen, Mechanism of Function of Viral Channel Proteins and Implications for Drug Development . In Kwang W. Jeon, editor: *International Review of Cell and Molecular Biology,* Vol. 294, Burlington: Academic Press, 2012, pp. 259-321.
ISBN: 978-0-12-394305-7

CHAPTER SIX

Mechanism of Function of Viral Channel Proteins and Implications for Drug Development

Wolfgang B. Fischer,* Yi-Ting Wang,* Christina Schindler,*,[1] *and* Chin-Pei Chen*

Contents

* Institute of Biophotonics, School of Biomedical Science and Engineering, National Yang-Ming University, Taipei 112, Taiwan
[1] Current address: Department of Physics and Astronomy, Heidelberg University, Germany

International Review of Cell and Molecular Biology, Volume 294
ISSN 1937-6448, DOI: 10.1016/B978-0-12-394305-7.00006-9

Abstract

Viral channel-forming proteins comprise a class of viral proteins which, similar to their host companions, are made to alter electrochemical or substrate gradients across lipid membranes. These proteins are active during all stages of the cellular life cycle of viruses. An increasing number of proteins are identified as channel proteins, but the precise role in the viral life cycle is yet unknown for the majority of them. This review presents an overview about these proteins with an emphasis on those with available structural information.

A concept is introduced which aligns the transmembrane domains of viral channel proteins with those of host channels and toxins to give insights into the mechanism of function of the viral proteins from potential sequence identities. A summary of to date investigations on drugs targeting these proteins is given and discussed in respect of their mode of action *in vivo*.

Key Words: Viral channel proteins, Viruses, Ion channels, Toxins, Membrane protein structure, Antiviral drugs.

1. Introduction

The cellular life cycle of viruses is tightly connected with lipid membranes. During viral entry, membranes have to be crossed, and within the cell, the viral life depends on subcellular membranes, since viruses build their proteins along lipid membranes. They also use the principle of compartmentalizing for optimized replication and therefore deform subcellular membranes. Another strategy is to capitalize on electrochemical and substrate gradients formed across membranes. For the use of these gradients in the most sensible way, channel-forming proteins are encoded in the genome of the virus. Channel-forming proteins are active at almost every stage of the viral replication. They are involved during the entry phase of the virus into the host and also within the infected cell. While the roles of some channels are well identified, for others this role still has to be elucidated. The assumption that similar tasks on a molecular level can only be accomplished by the same type of molecule in almost the same conformational and spatial arrangements inspires this review on the mechanism of function of viral channels in comparison with host channels.

What makes knowledge of the mechanism of function so important? There is the obvious reason that we are simply curious about it. One simply cannot stop wondering how mechanics can be achieved in an environment in

which we have to leave the concepts of movements in viscous media and can only rely on electrostatic and quantum mechanical principles to get a glimpse of what is happening. Learning more about the time domain of the mechanics is highly desirable as well. Maybe we can understand the biological "nano-machines" and design new ones, which are "longer lasting," capable of handling bigger loads, and show other improved characteristics. Since the viral channel-forming proteins are smaller than their host companions, their architecture depicts miniature design in an already miniaturized world, or going down-scale in an already down-scaled world.

On the other hand, there is crucial wish to secure and cure our health as well as to ease our life. How does knowledge about the mechanism of function fit into this wish? If we know the function of an enzyme, which cleaves a specific substrate, we can design a substrate which cannot be cleaved but rather jammed into the active site of the enzyme. If we know the conformation transition the molecule undergoes, we are able to generate more potent drugs. Dealing with other proteins than enzymes, such as the channel proteins mentioned here, the site of drug action is not so easy to elucidate. In principle, we "see" the protein but do not know where to go with our drug molecule. Consequently, an active site may be one of the many conformations the protein adopts during its "working cycle." From this particular perspective, one has to explore the entire conformational space of the protein as a prerequisite for improved drug development. Crystal structures serve as an important starting point for computational drug development representing "frozen" conformations. Computational modeling is able to screen and visualize more conformational space and in this respect possibly "link" individual crystal structures.

The idea is to analyze the viral channels in respect to larger host channels. Therefore, the architecture of those channels, which are anticipated to have a relation to the viral channels, is introduced. The relation is driven by sequence alignment of viral channel forming proteins (VCPs) with those of host proteins (Fischer and Hsu, 2011). Identifying related host proteins, specifically gating mechanics are elucidated and cross-related to the viral channels. In general, there are several mechanical movements especially within the lipid membrane known for ion channels, such as moderate conformational changes (Cymes and Grosman, 2008; Miyazawa et al., 2003; and references therein) and sliding of helices (Chang et al., 1998; Kuo et al., 2003). Openings of pores designed by toxins seem to be made irreversibly by assembly (Mueller et al., 2009). Finally, the idea of "drug hunting" is outlined in respect to small molecule drugs and peptide drugs.

The proteins are introduced with respect to the mechanism of function. All citations are driven by the idea to deliver structural information. For extended references about molecular biological information, it is referred to respective reviews. The work on viral channel-forming proteins has been reviewed in great detail in the literature (Fischer and Sansom, 2002;

Gonzales and Carrasco, 2003; and referenced literature below). Generally, the name "viroporin" or "VCP" is established in the literature for this class of proteins. So far, some of the channels are very selective for protons, others are permeable for small molecules, while the majority though are weakly selective for ions.

As to date, the biophysical role of the VCPs can be summarized to alter electrostatic repulsion of proteins so that lipid membranes can approach each other during fusion and budding, as well as alteration of cell homeostasis and membrane depolarization induced cell apoptosis (Franco and Bortner, 2006).

2. Viral Channel Proteins

VCPs comprise a series of proteins with different transmembrane (TM) topology. With the discovery of M2 from influenza A and Vpu from human immunodeficiency virus type 1 (HIV-1), proteins with a single TM topology have been found. Later, proteins such as 2B from Polio virus and p7 from hepatitis C virus (HCV) have been proposed to harbor two transmembrane domains (TMDs). The recently suggested viral ion channel from severe acute respiratory syndrome coronavirus (SARS-CoV), 3a, is now the longest channel with three TMDs. Other proteins found to form channels are belonging to either one of these classes of channels.

How can a protein be defined as a channel? Channels are made of subunits of proteins forming a circular tertiary structure around a symmetry axis. The channels *per se* could be either homo- or hetero-oligomeric. They are membrane embedded and conduct more or less selectively either one of the physiological relevant ions. The degree of selectivity comes with the diameter and side chain composition of the pore formed by the assembled proteins, the lumen of the pore. The wider the pore is, the less selective it should be. Less selective channel proteins are likely to be called pores (Gonzales and Carrasco, 2003), such as, 2B from Polio virus, which is able to conduct besides ions also small molecules.

In the following, the focus is on those VCPs for which detailed structural information is available either from experiments or from computational studies.

2.1. M2, Vpu, and p7

2.1.1. M2 from influenza A

The genome of influence is spread over eight single-stranded RNA segments. On the seventh segment, which encodes the matrix protein M1, a second overlapping reading frame has been identified coding a protein of about 11

kDa called M2 (Allen et al., 1980; Lamb and Choppin, 1981; Lamb and Lai, 1981; Winter and Fields, 1980) (Fig. 6.1A). Its topology is found to be monotopic comprising an N terminal side on the extracellular side marking it a type III integral membrane protein present at the plasmamembrane of infected cells (Lamb et al., 1985). The amino acid distribution indicates about 18–23 amino acids on the extramembrane side, 19 amino acids membrane spanning, and 54 amino acids toward the C terminus (Zebedee and Lamb,

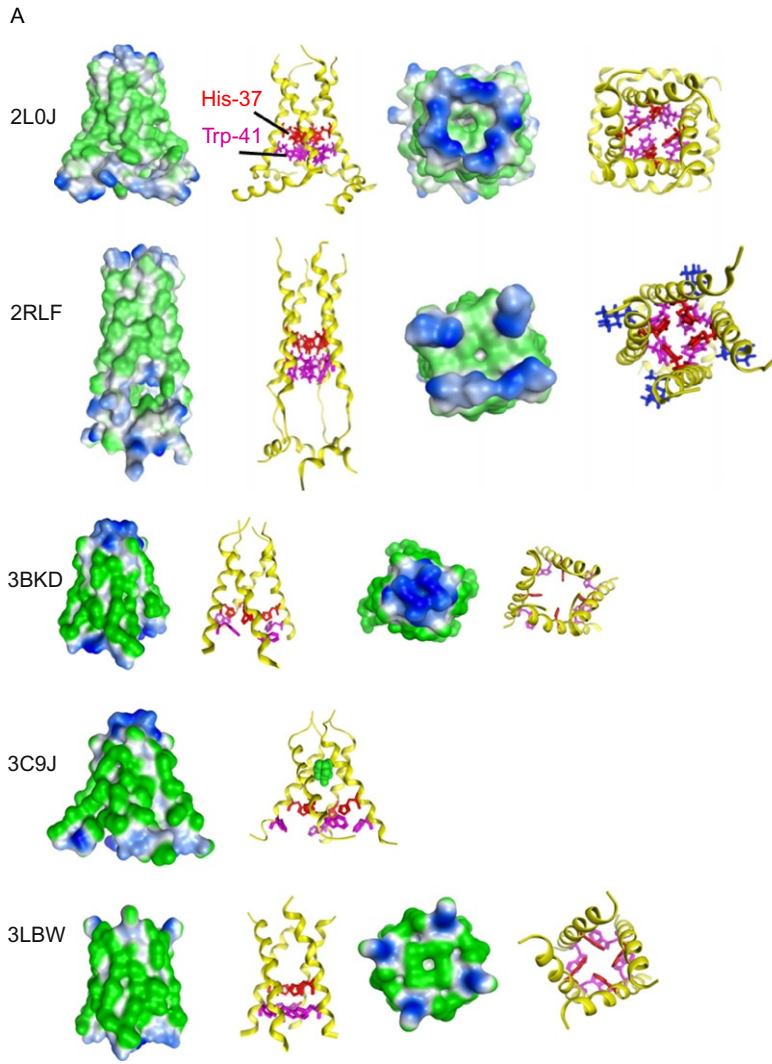

Figure 6.1 (Continued)

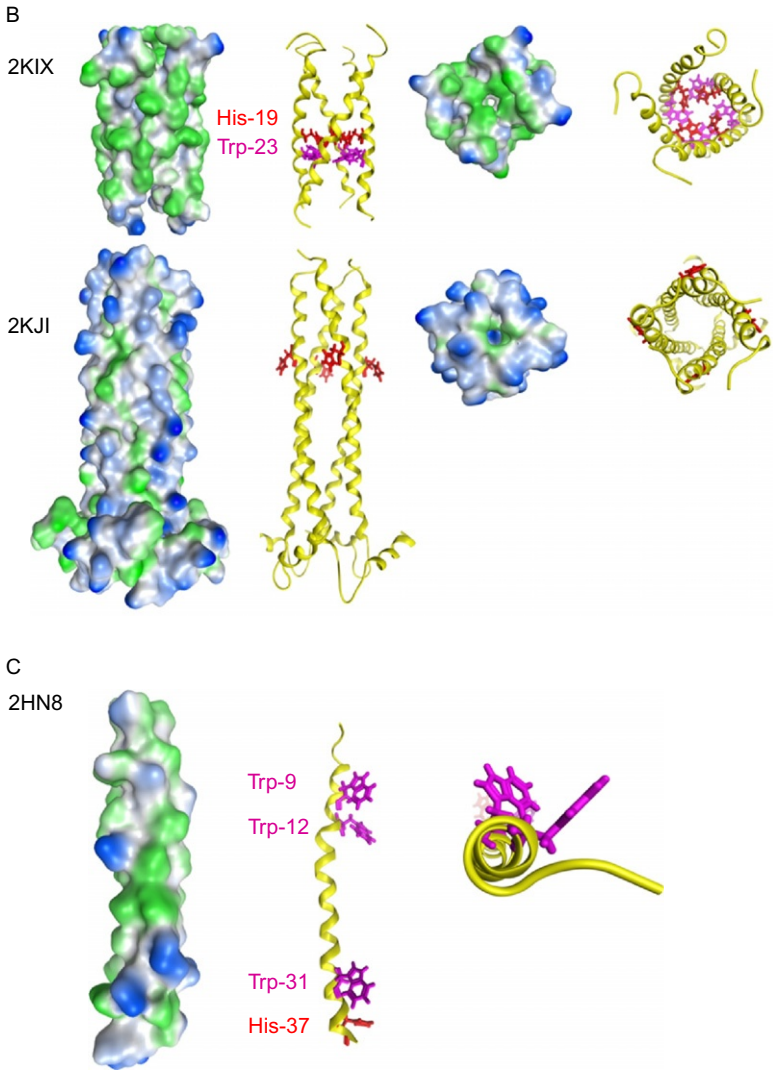

Figure 6.1 Available structures of M2 and BM2 from experimental sources. The structures are shown in "Gaussian Contact Mode" (MOE software) indicating hydrophilic residues in blue and hydrophobic residues in green. In addition, helices are shown as yellow bands and specific amino acids are represented in a stick modus (histidines in red and tryptophans in violet). (A) M2 channel: 2L0J from solid state NMR (Sharma et al., 2010); 2RLF from solution NMR (Schnell and Chou, 2008), the drug rimantadine is shown in stick modus (blue); 3BKD from X-ray and expressed protein (Stouffer et al., 2008); 3C9J from the same source as 3BKD with the drug amantadine shown in stick modus (green); 3LBW from SPPS (Acharya et al., 2010, from SPPS); (B) TMD (2KIX) and cytoplasmic domain (2KJ1) of BM2 (Wang et al., 2009b). (C) Structure of a synthetic peptide corresponding to PB1-F2 solved by NMR spectroscopy (Bruns et al., 2007).

1988). It is also present in the virion with about 14–68 molecules (Zebedee and Lamb, 1988). M2 assembles into cystein-linked homodimers which noncovalently associate into homotetramers (Holsinger and Lamb, 1991; Sugrue and Hay, 1991). Some of the M2 proteins of various subtypes have been identified to be palmitylated at Cys-50 (Sugrue et al., 1990). Amantadine resistance mutant studies of influenza viruses correlated resistance to mutations in the seventh segment, especially to the TMD of M2 (Hay et al., 1985). Mapping the mutations on a helical wheel reveals that the mutations are along one side of the helical structure. The mapping supports the idea that the protein assembles around a kind of central axis which is relevant for its functioning as a proton channel (Sugrue and Hay, 1991).

Experiments with a synthetic peptide construct representing the TMD of M2 reconstituted into artificial bilayers have verified its proton activity (Duff and Ashley, 1992). Also, whole-cell recordings of M2 and mutant M2 expressed in *Xenopus laevis* show that M2 activity is enabled by low pH and that amantadine is interacting with the channel (Wang et al., 1993). Channel activity has also been demonstrated in mammalian cells (Wang et al., 1994) and vesicle-based fluorescence essays (Schroeder et al., 1994), with the latter technique confirming proton conductance (Lin and Schroeder, 2001). Reconstitution of the protein into artificial bilayers also reveals channel activity of M2 (Tosteson et al., 1994). Electrophysiological experiments with M2 in mouse erythroleukemia cells have been conducted on ion selectivity confirming that M2 is 10^7 times more selective for protons than for monovalent cations (Chizhmakov et al., 1996). Whole-cell recordings with M2 expressed in *Xenopus* oocytes reveal a very low conductance of about 1–10 fA, which allows about 104 protons per second to pass (Mould et al., 2000). These measurements are flanked by results from studies with *X. laevis* (Shimbo et al., 1996). Using the whole-cell patch clamp technique on *X. leavis*, first evidence is given that the protonation state of the one histidine within the TMD is important for conductance (Wang et al., 1995). Proton conductance of full-length M2 expressed in BL21 cells and reconstituted into liposomes has also been shown to be independent on the presence of electrolytes (Vijayvergiya et al., 2004).

Using a fluorescence essay based study, it is reported that proton conductance is independent of the content of cholesterol in the liposomes (Lin and Schroeder, 2001). With this finding, it is proposed that M2 is active in lipid raft free environment and would just be associated with a lipid raft due to its cytoplasmic part. The authors suggest that raft association may control the number of M2 proteins to be incorporated into the virion.

Experimental evidence that the TMD of M2 is helical has been achieved with M2 peptide reconstituted into DOPC liposomes using CD spectroscopy (Duff et al., 1992). Solid NMR spectroscopic measurements with M2-TMD peptides confirm the helical motif, deliver tilt angles of the peptide within DMPC bicelles of about 33°, and suggest a left-handedness

of the putative bundle (Kovacs and Cross, 1997). By adding data from functional studies like Cys scanning and electrophysiological measurements as mentioned (Pinto et al., 1997) as well as computational modeling data (Sansom and Kerr, 1993; Sansom et al., 1997; Zhong et al., 1998), an approximate structural model of the tetrameric assembly of the TMDs of M2 with the histidines and tryptophans as important pore lining residues has been generated. In a combined study using FTIR spectroscopy with site-specific labeled amino acids and a dynamic molecular global search protocol, further strong support for the tetrameric model has been achieved (Kukol et al., 1999).

Extensive solid state NMR spectroscopic investigations on chemically synthesized TMD peptides of M2 delivered "high-resolution" distance and orientation data sets of the residues at pH 7.0 (Nishimura et al., 2002). A precise proposal has been given for the orientations of the tryptophans and histidines in a tetrameric assemble. In addition, helix stability has been confirmed. According to models of assembled helices, a water filled cavity toward the N terminal side has been suggested. Solid state NMR measurements of full-length M2 expressed in *Escherichia coli* and reconstituted into DMPC bicelles confirm the findings on the studies with peptides (Tian et al., 2002, 2003). These studies indicate a mode of assembly of the TMDs which is independent of the rest of the protein (Wang et al., 2011).

Studies based on tryptophan fluorescence on fully expressed M2 and mutants reveal that Trp-41 and His-37 work in concert upon low pH activation (Czabotar et al., 2004). Together with other experimental (Pinto et al., 1997; Wang et al., 1995) and computational studies (Sansom et al., 1997; Schweighofer and Pohorille, 2000), it is proposed that several mechanisms of function shuttle the proton across a selective and narrow part around the histidines of the channel. In one mechanism, called "shuttle" mechanism, the incoming proton is taken up by His-37 on its δ-nitrogen which induces a release of the hydrogen on the ε-nitrogen. Via a tautomerization, the sidechain of His-37 is reloaded. In another mechanism, the "water-wire" mechanism, the protonated histidines will repel each other allowing for an opening and transport via a hydrogen wire. Computational modeling combining classical molecular dynamics simulations with multi-state empirical valence bond (MS-EVB) approach (Schmitt and Voth, 1998) has shown that a hydronium ion will not move through the histidine ring. It is rather anticipated that the proton could shuttle even if the histidines are not fully removed to generate a kind of "open" channel (Smondyrev and Voth, 2002). The consequence of this study is that not all of the histidines need to be protonated and consequently charged to generate an "open" channel. Solid state NMR spectroscopic investigations have shown that at high pH, the channel can exist in a closed state when a neighboring pair of the histidines share a proton, and consequently, a third one releases this pairing and opens for a putative water-wire to conduct the proton

(Hu et al., 2006). With the detection of conformational distinct tryptophans upon low and high pH conditions by 19F NMR spectroscopy, a contribution of Trp-41 during channel gating has been verified (Winter et al., 2008). Finally, to date a cooperative gating model is proposed in which upon low pH on the N terminal side one histidine gets trapped via a cation–π interaction with the tryptophan while the other histidine is able to offer one of its protons to the water on the C terminal side (Sharma et al., 2010).

Structural models at atomic resolution are available based on NMR spectroscopy (Pielak and Chou, 2010; Schnell and Chou, 2008) and X-ray crystallography (Acharya et al., 2010; Stouffer et al., 2008; Wang et al., 2011) (Fig. 6.1A). All structures reveal a left-handed bundle. For the NMR investigations, a TMD M2 construct with an amphiphatic helix at the C terminal side has been used to stabilize the helix bundle which otherwise could not have been investigated (Schnell and Chou, 2008). The expressed M2 construct is reconstituted into DHPC detergent micelles and due to solution NMR spectroscopic investigations at high pH (pH 7.5). The construct is recorded in the presence of the antiviral drug rimantadine which interacts with the helix bundle at the lipid protein interface. The bundle forms a narrow pore which has a wider pocket of about 0.6 nm around Gly-34 and is highly restricted around His-37 and Trp-41. The structure is referred to as a potential closed form of the channel (Pielak and Chou, 2010). Solely, the TMD of M2 has been crystallized and its structure resolved to 0.2 nm in octyl-β-D-glucopyranoside (OG) detergents at high pH (pH 7.3) (Stouffer et al., 2008). The pore is opened into a tepee-like shape with its restriction on the N terminal side and the Trp-41 apart from each other. A mutant M2 (Gly-34 is replaced by alanine) cocrystallized with amantadine at lower pH (pH 5.3) identifies a structure which is similar in shape as the one crystallized at pH 7.3. The binding site of amantadine is marked to be within the lumen of the pore. The shape of the bundle is considered to represent an open form of the channel. Solution NMR studies reveal that at low pH the TMDs are dynamic (Hu et al., 2011; Li et al., 2007; Pielak et al., 2009). It is a common theme of all models that, besides the His-X-X-X-Trp motif, Asp-44 and Arg-45 play an additional role in the gating mechanism.

Similar to influenza A, segment 7 of the influenza B genome also harbors two proteins M1 and M2 with the latter to be a proton channel called BM2 (Briedis et al., 1982) of about 15 kDa (109 amino acids) (Horvath et al., 1990). The sequence of BM2 is highly conserved which indicates its importance for the virus (Hiebert et al., 1986). The protein is phosphorylated and localized in the cytoplasm but also transported to the plasma membrane where it is incorporated into virions (Odagiri et al., 1999). Like M2, BM2 is a type III integral membrane protein with an H-X-X-X-W motif but with no further sequence homology with M2 including cysteins in the ectodomain (Paterson et al., 2003). Its role is suggested to

equilibrate the pH gradient between the Golgi and the cytoplasm by forming proton channels (Mould et al., 2003). Proton conductance of BM2 is found to be higher than for M2. Mutation studies identify polar serine residues (serines 9, 12, and 16) facing the lumen of the pore which is discussed as an explanation for the resistance of BM2 against amantadine (Ma et al., 2008; Paterson et al., 2003). The oligomerization state is experimentally confirmed to be a tetramer together with functional studies using the two electrode voltage clamp method (Balannik et al., 2008). Despite functional similarity with M2 protein, BM2 cannot form oligomers with M2. Not forming a tetramer via the "dimer of a dimer" concept, the route of assembly seems to follow the same as for other VCPs such as Vpu, p7, or 2B.

Solution NMR spectroscopy identifies a large left-handed coiled-coil tetramer consisting of two segments, separated by a 10-amino-acid region (residues 34–43) (Wang et al., 2009b) (Fig. 6.1B). The "full-length" structural model is derived from experimental results of two overlapping constructs: a TMD containing construct $BM2_{1–33}$ (2KIX) and a cytoplasmic domain containing construct $BM2_{26–109}$ (2KJ1). With its large cytoplasmic domain which generates a large dipole moment, it is suggested that BM2 is also involved in the recruitment of matrix proteins at the cell surface and in combination with that involved in the viral assembly and budding process. The channel domain consists of two heptad repeats Leu-8 to Ile-14 and Leu-15 to Ile-21, and the data confirm serines 9, 12, and 16 as pore lining. Ser-12 completely faces the pore while the other two are also involved in interhelix packing. The pore is occluded by a ring of four Phe-5 and Trp-23. Interesting to note is that mutations of Ser-12 and Ser-16 into alanines affect proton conductance much more than mutations of His-19 and His-27 into alanine (Wang et al., 2009b). Computational modes of the TMDs of BM2 have been modeled using coarse-grained simulation techniques in combination with united atom simulations (Rouse et al., 2009). The suggestion in this study is that, also in this channel, a minimum of three histidines need to be protonated to induce conformational changes which lead to an open conformation.

Antiviral amantadine does not inhibit the activity of BM2 (Paterson et al., 2003). The reason is found to be due to the polar serines facing the lumen of the pore. More polar drugs seem to be necessary to block the channel (Ma et al., 2008). Recently, a monoclonal antibody has been identified to target the ectodomain of BM2 comprising antiviral activity successfully (Wang et al., 2010b).

With PB1-F2 encoded by influenza A, a second channel protein has recently been identified (Chanturiya et al., 2004; Henkel et al., 2010) of which a structural model for its TMD is reported (Bruns et al., 2007) (Fig. 6.1C). This protein has been found with a strong tendency to oligomerize. This would be the second virus, next to SARS-CoV which encodes more than one channel protein. The studies have been done with synthetic

peptides reconstituted into planar lipid bilayers and microsomes. The structural integrity has been demonstrated with a united atom MD simulation in a fully hydrated lipid bilayer.

To date, investigations on M2 are very advanced in respect to structural and functional studies. Albeit, structural information about the cytoplasmic domain is still lacking, the TMD is very well characterized by NMR and X-ray data. The protein has been for a long time a potent drug target (Davies et al., 1964).

2.1.2. Vpu from human immunodeficiency virus type 1

In the late 1980, a novel open reading frame hosting a 16-kDa protein has been detected independently by two groups (Cohen et al., 1988; Strebel et al., 1988) (Fig. 6.2). The protein has been called Vpu. Upon introduction

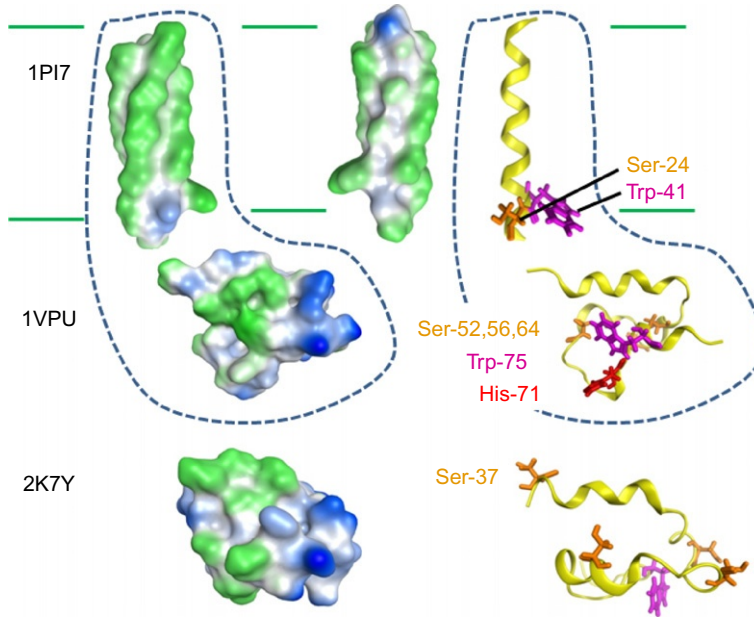

Figure 6.2 Available structures of Vpu from experimental sources. The structures are shown in "Gaussian Contact Mode" (MOE software) indicating hydrophilic residues in blue and hydrophobic residues in green. In addition, helices are shown as yellow bands and specific amino acids are represented in a stick modus (histidines in red, tryptophans in violet, and serines in orange). 1PI7 TMD from solid state NMR (Park et al., 2003), 1VPU (Willbold et al., 1997) and 2K7Y (Wittlich et al., 2009) are structures derived from solution NMR. The dashed lines should indicative for the whole protein.

of a frame shift mutation into the Vpu gene, an up to 10-fold reduction of viral load has been observed (Strebel et al., 1988). The conclusion drawn from the experiments has been that Vpu is involved in virus assembly and particle release. The new protein has not been detected in HIV-2 and SIV (Cohen et al., 1988).

Vpu's involvement in inducing particle release (Strebel et al., 1988, 1989; Terwilliger et al., 1989) has been attributed to a downregulation of the receptor protein CD4 via the proteasome pathway (Ruiz et al., 2010a; Willey et al., 1992a,b) and the formation of ion channels (Ewart et al., 1996; Schubert et al., 1996b). The two routes of action are attributed to two distinct domains of the protein (Schubert et al., 1996a): the cytoplasmic domain for the former (Bour et al., 1995) and the TMD for the latter (Schubert et al., 1996b). The mechanism of how the protein enhances virus particle release is anticipated by the formation of a homooligomer at the site of the plasma membrane which renders the membrane permeable for ions (Schubert et al., 1996b).

CD4 degradation is found to be due to the interaction of a short sequence, KRLLSEKKT, in the cytoplasmic tail of CD4 with a helical domain of the cytoplasmic part of Vpu (Tiganos et al., 1997). Also, residues at the linker region between the TMD and cytoplasmic domain of Vpu contribute to CD4 degradation (Tiganos et al., 1998). For CD4 downregulation, the two phosphorylation sites of Vpu, Ser-52 and Ser-56, are identified to be essential (Paul and Jabbar, 1997; Schubert et al., 1994). Downregulation via interaction with Vpu has also been reported for βTrCP (Margottin et al., 1996) to hand over CD4 to the proteosomal degradation pathway. Also, other host proteins such as Vpu binding protein (UBP) (Callahan et al., 1998), CD74 (Hussain et al., 2008), and CD317 (Bolduan et al., 2011; Neil et al., 2008; van Damme et al., 2008) are "marked" by Vpu for downregulation. Interaction of Vpu with host factors at the site of the plasmamembrane are reported for TASK channels (Hsu et al., 2004) and BST-2/tetherin (also called CD317) (Neil et al., 2008; van Damme et al., 2008). In both host proteins, the TMD of Vpu is responsible for the interaction (Hsu et al., 2004; Skasko et al., 2011). For BST-2, it has been shown that Vpu slows down BST-2 transport to the plasma membrane (Dubé et al., 2010) and that the Vpu-BST-2 complex is retained in the ER (Skasko et al., 2011). The interaction is reported to be due to the TMDs of both proteins. BST-2 itself is known to form a dimer and crystallographic data identify for the extramembrane part an elongated helical motif which forms a coiled-coil toward the C terminal side and a flexible region able to assemble into a tetramer on the N terminal side (Hinz et al., 2010; Schubert et al., 2010).

The loop sequence, EYRKLL, connecting the TMD of Vpu with its cytoplasmic domain has been shown to be responsible of transporting Vpu to the plasma membrane (Ruiz et al., 2008). At the site of the plasma

membrane, it is anticipated that Vpu forms channels via oligomerization. Expression of Vpu in amphibian oocytes induces conductance of cations measured under voltage clamp conditions (Coady et al., 1998; Schubert et al., 1996b) which shows marginal effect on divalent ions such as Ba^{2+} and Ca^{2+}. Together with peptides representing the TMD and a scrambled sequence, it has been shown that solely the TMD exhibits cation specific channel activity. A series of experiments has been performed which show that expressed Vpu in *E. coli* purified and reconstituted into artificial bilayers exhibit channel activity (Ewart et al., 1996; Mehnert et al., 2007). Recordings solely with the TMD of Vpu reveal similar conductivity compared to full-length protein with minimal changes in the kinetics (Ma et al., 2002; Mehnert et al., 2007). Replacing Trp-23 by Leu in a synthetic peptide construct, Vpu_{132}, reconstituted into artificial lipid bilayers, alters the open time duration and shut kinetics of the peptide, while a change of Ser-24 to Leu abolishes channel activity completely (Mehnert et al., 2008). No affect has been reported when Arg-31 is exchanged into Val. Channel recordings of the TMD of Vpu in solutions of different ions reveal that the Vpu channels which are only slightly selective indicate almost pore-like characteristics. It has been suggested that Vpu shows a channel-pore dualism (Mehnert et al., 2008) which means that Vpu can either act as a more or less selective channel or non-selective pore depending on specific *in vivo* conditions. These conditions could possibly be due to changes in lipid environment. In a recent electrophysiological study, using whole-cell clamp conditions with 293T cells expressing full-length Vpu mutant S24A does also not exhibit channel activity (Bolduan et al., 2011).

In another study, in which Vpu has been expressed in *E. coli*, the protein renders the membrane of the cells susceptible to a series of molecules as well (Gonzales and Carrasco, 1998). 2-Nitrophenyl-D-galactopyranoside, uridine, translation inhibitor hygromycin B, and lysozyme are reported to pass the membrane as well as hygromycin B and neurobiotin when expressed in eukaryotic COS cells.

Channel activity allows the change of electrochemical gradients, depolarization, across the lipid membrane. The effect of depolarization of the membrane is reported to affect the fission of the budding HIV-1 virion from the infected HeLa cells (Hsu et al., 2010) (e.g., lowering electrostatic repulsion to enable fission): Blocking two-pore K^+ (K_{2P}) channel TASK virion release with Vpu inactive HIV leads to an enhancement of virion release. Since TASK channel activity in HeLa cells measured under whole-cell voltage clamp conditions is not affected in the presence of Vpu, it is concluded that Vpu reduces the number of TASK channels at the plasma-membrane by interacting with the K^+ channel making it susceptible for degradation. Sequence similarity of the TMD with the first TMD of TASK implies physical interaction of the two proteins (Hsu et al., 2004).

It can be concluded at this state that Vpu interacts with host proteins, which leads to downregulation via the proteasomal pathway or redirecting them. Consequently, channel activity of Vpu *per se* does not seem to be necessary to fulfill its auxiliary role in enhancing viral release. Yet, Vpu especially when inserted into lipid membranes shows channel activity which can be modulated by mutations. Escape mutant studies as done for M2 from influenza A (Hay et al., 1985) are lacking and a selective "channel blocker" is not yet identified (Lamb and Pinto, 1997). The recent anti-channel drug BIT225, *N*-[5-(1-methyl-1*H*-pyrazol-4-yl)-naphtalene-2-carbonyl]-guanidine, seems to fulfill the role as a Vpu channel blocker when administered in a concentration of 40 μM to Vpu reconstituted into artificial lipid membranes of a channel recording device (Khoury et al., 2010).

Structural information of Vpu has emerged from solution and solid state NMR spectroscopy (Fig. 6.2). In the late 1990s, two structural models of the cytoplasmic domain of Vpu have been published using solution NMR spectroscopy (Fig. 6.2). The structural features discovered have been a helix–loop–helix motif followed either by another short helix (Willbold et al., 1997) or a reverse turn (Federau et al., 1996; Wray et al., 1995). While the former data derived from recordings of Vpu expressed in *E. coli* purified and dissolved at high salt solution, the latter spectra have been recorded from a synthetic peptide dissolved in aqueous TFE solution. It is debated that the high salt solution induces the tertiary fold and thus the formation of the third helix. TFE is known to support helix formation but weakens the formation of a fold. More recent data in low salt solution confirm two helical motifs in the cytoplasmic domain (Wittlich et al., 2009). Measurements in the presence of micelles formed by dodecylphosphatidycholine (DPC) induce secondary elements (two helices) and a tertiary fold. Secondary structures are supported by CD spectroscopy (Wittlich et al., 2009; Wray et al., 1995). All structural investigations have in common that the two series 52 and 56 have not been phosphorylated. Investigations on the structural implications of phosphorylation of the two serines to the structure have been done either on a synthetic peptide in aqueous TFE solution (Coadou et al., 2001, 2002) or on a peptide expressed in *E. coli*, purified and measured in the presence of DPC micelles (Wittlich et al., 2008). Without DPC upon posphorylation, parts of the cytoplasmic helices unwind into a β-strand (Coadou et al., 2002), while in the presence of DPC micelles, structural changes are limited to some loss of helicity of helix1 toward the C terminus and extension of helicity toward the N terminal side of helix2 (Wittlich et al., 2008).

The helix motif for the TMD of Vpu has first been suggested by solid state NMR spectroscopy (Marassi et al., 1999; Wray et al., 1999). Applying the same technique to extended constructs of the TMD of Vpu with residues of the cytoplasmic domain indicates that the second helix is aligned

parallel to the membrane surface (Marassi et al., 1999; Park et al., 2003). X-ray reflectivity measurements done with full-length Vpu on a lipid monolayer reveal that the second helix in the cytoplasmic domain is bound loosely (Zheng et al., 2001). The helical motif of the TMD of Vpu has been supported by site-specific FTIR spectroscopy (Kukol and Arkin, 1999). SSNMR data show that the TMD Vpu construct shows rotational dynamics within the lipid membrane (Park et al., 2006). The extent of the TMD helix is still controversial, when comparing all the SSNMR data. In a recent study, the length of the helical motif toward the C terminal side of the TMD is reported to extend beyond the hydrophobic slab of the bilayer (Sharpe et al., 2006).

The TMD of Vpu is found to exhibit a weak kink around Ile-17, a result obtained using a Vpu_{2-30+} construct measured by solid state NMR spectroscopy (Park et al., 2003). MD simulations using a Vpu_{1-52} construct support the findings reporting kink angles to vary between 7° and 15° around the same amino acids found experimentally (Sramala et al., 2003). Computer simulations in various lipids identify a kink around Ser-24 due to the compensation of hydrogen bonding of the side chain with adjacent backbone residues toward the N terminal side (Krüger and Fischer, 2008). Further bending of the helix is found from Ser-24 to Ile-20. Kinking is seen as a mechanism to compensate for varying lipid thicknesses. To summarize the findings, there could be hinge regions around Ile-17 and Ser-24 proposing modular segments of the protein within the lipid bilayer.

According to the hypotheses of Vpu being released after manufacturing into the ER membrane, the protein could oligomerize prior to any interaction with other host proteins. Oligomerization is also seen as a prerequisite of channel formation. Earliest studies point toward an oligomeric assembly using SDS-PAGE (Maldarelli et al., 1993). On the bases of synthetic peptides linked together as either tetramers or pentamers and their channel activity, the latter state is reported to be the favored one (Becker et al., 2004). Full-length Vpu and its TMD alone, both expressed *in vitro* and analyzed using gel permeation chromatography, are found to be in a pentameric state (Hussain et al., 2007). Computational modeling of the TMD based on SSNMR data on expressed TMD of Vpu supports the pentameric state (Park et al., 2003) but a tetrameric state is also proposed. A combined experimental study using bilayer recordings on synthetic peptide based on the TMD and computational modeling using MD simulations is in favor of the pentameric assembly (Cordes et al., 2002).

Pentameric assemblies have been used for the computational modeling of the Vpu ion channel embedded in hydrated lipid bilayers (Cordes et al., 2001; Grice et al., 1997; Moore et al., 1998). Simulations of hexameric assemblies in a hydrated slab of octan, mimicking a lipid bilayer, have been reported to collapse and are disregarded as a potential assembly

(Lopez et al., 2002). In another simulation study in a hydrated POPC bilayer system, the tetrameric and hexameric assemblies have been ruled out based on the derived pore radii and the estimated conductance these pores would show (Cordes et al., 2002). Simulations on extended models including the first cytoplasmic helix (Sramala et al., 2003) and the entire cytoplasmic part have been reported with the proteins embedded either in a lipid monolayer at the air water interface (Sun, 2003) or in hydrated POPC (Lemaitre et al., 2006; Sramala et al., 2003). In one simulation of full-length Vpu, the cytoplasmic domain has been generated artificially based on the available NMR data (Sun, 2003) while for the other simulations experimentally derived cytoplasmic domain data have been artificially merged with simulated extended Vpu (Lemaitre et al., 2006; TMD and first cytoplasmic helix taken from Sramala et al., 2003).

Vpu is predominantly acting via interactions with other host proteins. Structural information of the TMD is in lack of X-ray crystallographic data, but in contrast to M2, the structural details of the cytoplasmic domain are well resolved. Ion channel functionality is still being debated and it seems that Vpu may emerge as a potential drug target.

2.1.3. p7 from Hepatitis C virus

The genome of HCV is expressed as a large polyprotein and cleaved by cellular and viral proteases into 10 cleavage products among which is p7, a 63 residue 6–7 kDa bitopic membrane protein (Elbers et al., 1996; Lin et al., 1994) (Fig. 6.3). The protein is preceded by the structural protein E2 from which it is incompletely cleaved and succeeded by the nonstructural protein NS2. It is not clear at this moment to which side structural or nonstructural p7 belongs to. Abolishing the cleavage between E2 and p7 results in noninfections virions (Harada et al., 2000). Expressing E2 and p7 independently recovers the production of infectious virions making p7 an essential part of the life cycle of HCV. Also, functional relevant interaction of p7 with NS2 has been reported (Tedbury et al., 2011). NS2 is located to sites where viral replication and particle assembly take place. In the absence of p7, the location of NS2 to these sites is lost. This function of p7 is reported to be independent of its function as a channel protein. It has been suggested that p7 plays an accessory role in altering the topology of NS2 which consequently affects NS2 function (Ma et al., 2011).

As a channel-forming protein, p7 is proposed to have the same role in the life cycle of the virus as M2 supporting cell entry (Griffin, 2009).

It has been discovered that p7 is necessary during the early stage of particle assembly (Jones et al., 2007; Steinmann et al., 2007a). Using a so-called J6/JFH chimeric genome which can be used to study the HCV life cycle in human hepatoma cells (Huh-7.5), it has been shown that p7, but not its precursor forms E2-p7 and p7-NS2, is required for infectious virus production (Jones et al., 2007). Mutations in the basic loop between the

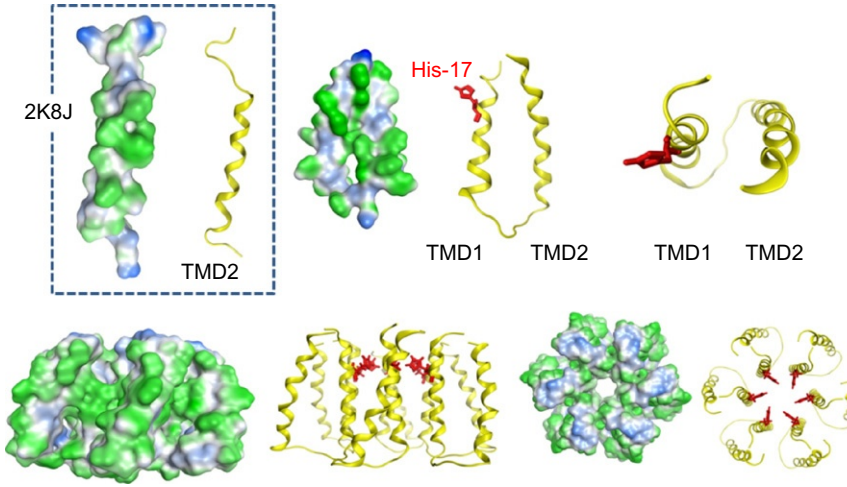

Figure 6.3 Available structure of p7 from experimental and computational sources. The structures are shown in "Gaussian Contact Mode" (MOE software) indicating hydrophilic residues in blue and hydrophobic residues in green. In addition helices are shown as yellow bands with histidine residue represented in a stick modus (red). 2K8J: TMD2 from solution NMR (Montserret et al., 2010), boxed; top row to the right is a computationally assembled monomer, lower row a potential hexameric assembly of the monomers forming a channel.

two TMDs (KR33/35QQ or KR33/35AA) lead to a decrease of the amount of released infectious virions (Steinmann et al., 2007a). It is proposed that these mutations affect channel activity as they are at the mouth of the putative pore. Other mutations within the TMDs of p7 (TMD1 and TMD2), such as the highly conserved Trp-30 and Tyr-42 each of them being separately mutated into phenylalanine, impair the infectivity of the virions. Mutations of His-31 also do not have an effect on RNA replication (Steinmann et al., 2007a), similar to the wild-type p7 (Lohmann et al., 1999). Concluding from these data, p7 is not essential for viral entry, supporting the essence of p7 within the later stage of infectivity which is linked to virus assembly. Nevertheless, p7 is essential for the virus but the mechanism of ion channel activity is not yet linked to either of these events.

The topology of p7 has been identified to contain two TMDs connected via a short hydrophilic segment. Both ends of the TMDs are found to point into the ER lumen (Carrère-Kremer et al., 2002). The protein is detected within the plasma membrane with both termini pointing toward the extracellular environment. Experiments with p7 expressed in *E. coli* (Clarke et al., 2006; Griffin et al., 2003), as well as p7 protein derived from solid phase peptide synthesis (SPPS) (Pavlovic et al., 2003; Premkumar et al., 2004), both individually reconstituted into artificial lipid bilayers disturb the

bilayer, making it susceptible to ion conductance. Most recent data reveal that channel activity is dependent on lipid composition and they are discussed together with data from CD in terms of a change in topology of the protein (Whitfield et al., 2011). It is proposed that a lipid dependent equilibrium between an antiparallel alignment and a L-shape alignment (one helix parallel the other perpendicular to the membrane normal) of the two TMDs exists.

In another study of p7 purified from the same expression system p7, it has been reported using transmission electron microscopy (TEM) that the protein assembles into a hexamer (Griffin et al., 2003). With a FLAG-p7 construct at the N terminal side also expressed in *E. coli*, purified and measured with TEM, a heptameric assembly is proposed (Clarke et al., 2006). The heptameric assembly has been supported by SDS-PAGE and mass spectrometry. Most recently, electron micrographs of p7 synthesized by SPPS are in support of a hexameric assembly of the protein (Luik et al., 2009).

The first computational model of p7 has been generated using a coarse grained conformational search protocol (Patargias et al., 2006) (see also Fig. 6.3). The two TMDs and the short link between them have been identified as a consensus from the results of multiple secondary structure prediction programs (Cuthbertson et al., 2005). The antiparallel aligned p7 protein is hither forth called the monomer. The alignment as a monomer positions the TMDs so that a bundle could be formed in which the histidines of TMD1 of all the monomers point into the putative lumen. Consequently, a pivotal role for this particular histidine in gating has been suggested (Patargias et al., 2006). Other groups have also challenged computational modeling to fill the data from electron microscopy (EM) with structural information (Griffin et al., 2003). Most recent MD simulation studies with an extended p7 protein randomly positioned in a simulation box together with lipid molecules using coarse grained techniques support the antiparallel alignment of the TMDs in the p7 monomer (Luik et al., 2009). The role of histidine in the conductance of ions across the protein bundle has been supported by mutant studies of chemical synthesized p7 reconstituted into lipid bilayers (Chew et al., 2009). Studies with Cu^{2+} containing solutions in combination with wild-type and H17A mutants have allowed the conclusion that histidine is pore lining, as predicted earlier (Patargias et al., 2006).

Solution NMR spectroscopic experiments with p7 expressed in *E. coli* and reconstituted into DHPC micelles deliver data which support its bitopic topology (Cook and Opella, 2010, 2011). Both of the two TMDs are split into two segments with specific dynamics comprising four helical segments. The two unstructured N and C termini as well as the short and mobile loop segment between the TMDs comprising residues 28–36 are outside of the membrane. Residues 5–15 constitute a helical segment embedded into the micelles which is similar to the third segment in its dynamics. While the first helix has no membrane anchoring amino acids, the third helical segments

including residues 41–48 seem to be affected by the dynamics of the loop segment. The second helix (residues 17–27) is found to be less mobile and it is suggested that this is due to the membrane anchoring aromatic residues Trp-30 and Tyr-31. Similarly, low mobility is also found for the fourth helix which is flanked by two prolines, Pro-49 and Pro-58, containing a stretch of five leucines (Leu-50–Leu-54).

In another solution NMR spectroscopic study, data of full-length p7 derived from peptide synthesis and recorded in a mixture of trifluoroethanol and water also mainly identify helical motifs (Montserret et al., 2010) (Fig. 6.3, boxed). Flexible regions around residues Gly-15 and Gly-18 of TMD1 and at the C terminal end of TMD2 are observed. CD measurements in various membrane mimetic environments support the overall helicity of the protein in its monomeric state. Distance restraints from the NMR measurements have been used as input for computational modeling using a docking approach in combination with extended molecular dynamics simulations to model the assembly of the two TMDs. The model reveals that the aromatic residues Phe-25, Trp-30, Tyr-42, Tyr-45, and Trp-48 form a staged π-system.

Channel characteristics of p7 reconstituted into asolecitin bilayers identify a voltage-dependent current behavior which is rectifying and showing an 11 times higher selectivity for cations (Montserret et al., 2010). Main conductance levels are reported to be 22 and 41 pS at +60 and +140 mV, respectively. Patch recordings with liposome identify slightly higher conductance levels at around 35, 57 120, and 184 pS when a pipette holding potential of +140 mV is applied. Channel recordings are reported to be blocked by hexamethylene amiloride (HMA) but not by amantadine. The pore lining TMDs is identified to be TMD1, since a major conductance level of about 60 pS has been found at a holding potential of +100 mV when reconstituted into lipid bilayers. In contrast, there could be no channel recordings observed for TMD2. A synthetic full-length p7 construct derived from SPPS shows a reversal potential of 44.3 mV in a 10:1 (*cis*:*trans*) gradient buffer, suggesting a moderate cation selectivity (Premkumar et al., 2004). The experiments indicate that the protein bundle shows lower permeability for calcium ions and considerable chloride conductance.

The oligomerization state of p7 is dependent on the protein:detergent ratio ($C_{12}E_8$) when using sedimentation experiments (Montserret et al., 2010). At lower ratio, a hexameric assembly is proposed which can shift to slightly higher numbers at higher ratios. So far, crystallization trials failed to deliver any conclusive structural information (Jones et al., 2007).

His-17 has been identified to point into the lumen of the pore (Patargias et al., 2006). This residue has also been found in M2, which is identified as proton sensor involved in gating of the channel. Conductance studies of p7 when reconstituted into artificial lipid bilayers reveal that the presence of Cu^{2+} in the bath solution blocks the activity of p7 (Chew et al., 2009).

Since copper ions can be complexed by histidines, this study confirms the orientation of these residues toward the pore. With histidines in the pore, it has also been suggested that this allows pH sensitivity in any kind of form (Patargias et al., 2006): is the p7 bundle just sensitive to protons but does not conduct them? Or is p7 also a proton conductor similar to M2? It has been now suggested that protonation of the histidines will lead to an opening of the pore (Foster et al., 2011). With further analogy to M2, the question arises, can the protein also be built by less than the six units as it is proposed to date? Of course, experimental evidence is given for larger units, such as hexamers and possibly heptamers.

2.2. Other channel-forming proteins

2.2.1. 6K from alphavirus

A series of proteins in other viruses have also been reported as VCPs (Carrasco, 1995; Fischer, 2005; Fischer and Sansom, 2002; Gonzales and Carrasco, 2003).

One of these proteins is 6K, which is found in several viruses of Alphavirus genus belonging to the family togaviridae (Carrasco, 1995; Garoff et al., 1982; Madan et al., 2005; Schlesinger and Schlesinger, 1986; Strauss and Strauss, 1994; Wang et al., 2010a). Alphaviruses express their structural proteins in a polyprotein consisting of E3-E2-6K-E1-C which is proteolytically processed into its constituents (Liljestrom and Garoff, 1991). The 6K protein is a 6 kDa hydrophobic protein of 60 amino acids which is palmitylated (Gaedigk-Nitschko et al., 1990; Lusa et al., 1991). It is found to be transported to the site of the plasma membrane via a p62/E1 complex and only to a lower extend incorporated into the budding virion (Lusa et al., 1991). Albeit site-specific mutation in the 6K region identifies viruses with reduced budding capabilities, a full deletion of the protein does not result in blocking viral replication. The lack of 6K leads to an altered spike structure of the virion and it is concluded that the protein is important for the correct assembly of the virion (McInerney et al., 2004). These findings make 6K another accessory protein which amplifies the release of virions. Two hydrophobic stretches in the sequence of 6K suggest two TMDs one of which would be long enough to span the bilayer (Liljestrom and Garoff, 1991). A bioinformatics approach using a hidden Markov model reduces the number to only one TMD (Sonnhammer et al., 1998). A single TMD is also the conclusion drawn from mutation studies of Semliki Forest virus 6K protein in its interfacial region (Sanz et al., 2003). Ross River and Barmah Forest virus 6K proteins expressed in *E. coli* and reconstituted into artificial lipid bilayers form channels with conductance ranging from 40 to 800 pS (Melton et al., 2002). The large conductance is attributed to the formation of larger oligomeric units of the protein. No other roles than permeabilizing the lipid membrane and being involved in the budding process are known to date.

It has been discussed that topology and mechanism of function of 6K is dependent on lipid thickness and constitution which the protein experiences during trafficking (Sanz et al., 2003), a mode of action which has also been suggested for Vpu from HIV-1 (Mehnert et al., 2008).

2.2.2. E, 3a, and 8a from severe acute respiratory syndrome-corona virus

Coronaviruses belong to the family of coronaviridae and replicate in various animal species (Marra et al., 2003; Stadler et al., 2003). Human coronaviruses have been known since the 1960s (Myint, 1995). In 2002, a member of the virus has been found to cross the species barrier and infected humans with a mortality rate of about 5%, and even higher for people above their sixties (Zhong et al., 2003). The symptoms are described by a SARS which are almost flu like and come with severe fever (Stadler et al., 2003). The name of the family derives from a corona like shape of the virion when observed in electron microscopy (Beniac et al., 2006). Coronaviruses belong to the enveloped viruses and harbor the largest positive-sense single-stranded RNA genome of 30–32 kb amongst the RNA viruses (Narayanan et al., 2008). The genome is transcribed into a large polyprotein which is cleaved by virus-encoded proteases. The structural proteins are spike (S), matrix (M), and nucleocapside proteins (N) as well as the envelope protein (E). A large series of accessory proteins is distributed toward the 3′ end of the genome (Narayanan et al., 2008) among several proteins exhibiting channel activity, as listed below.

Protein E has a length of 76 amino acids with a short N terminus of 7–9 amino acids, a long TMD of 21–29 amino acids and a C terminus (Shen et al., 2003). When E protein is synthesized and reconstituted into artificial lipid bilayers, channel activity with conductance in the range of 50 pS is observed (Wilson et al., 2004). SDS-PAGE experiments identify E protein to form pentamers (Parthasarathy et al., 2008). Electrophysiological measurements using whole-cell clamp conditions of E protein gene infected HEK-293 cells reveal a current which is sensitive to the administration of HMA (Pervushin et al., 2009). FTIR spectroscopic investigations suggest a helical hairpin-like structure for the long TMD of E protein (Arbely et al., 2004). It is argued that, the peptide is highly helical with hardly any tilt and has a phenylalanine (Phe-23) located toward the lipid head group region. In addition to that, an asparagine (Asn-15) would support the N and C terminal ends to assemble. NMR spectroscopic investigations support a helical TMD without any turns (Pervushin et al., 2009). Merely, a leucine residue (Leu-18) does not fit into the residual dipole coupling calculations proposing a non-helical section or a conformational flexible region. Computational modeling studies of the E protein in an implicit bilayer model using Monte Carlo simulations support the experimental results of the secondary structure of the membrane traversing helical domain to be helical

(Chen et al., 2010). The calculation starts from a random conformation of the TMD fully embedded in the hydrophobic slab of the bilayer. The presence of HMA differences in the 1HN chemical shifts of two residues on either side of the TMD is found when compared to those without any drug (Pervushin et al., 2009). This is in contrast to measurements in the presence of amiloride. Consequently, HMA is suggested to be located within the pore most likely at the C terminal mouth.

ORF 3a of SARS-CoV is another protein identified to exhibit channel activity when expressed in *Xenopus* oocytes (Lu et al., 2006). It is located between S and E proteins and built by 274 amino acids (Zeng et al., 2004). The protein is found at the site of the plasma membrane and in the cell (Tan et al., 2004; Yuan et al., 2005) as well as in intracellular virus particles (Ito et al., 2005; Yu et al., 2004; Yuan et al., 2005). The protein is also released in membranous structures from infected and 3a expressing cells (Huang et al., 2006). Similar to other channel-forming proteins of other viruses, 3a also interacts with a series of other host and viral proteins (Narayanan et al., 2008). Three TMDs are proposed at the N terminal side preceding a longer C terminal cytoplasmic domain of about 148 amino acids. Residues 127–133 harbor a cystein rich region which is involved in connecting to monomeric 3a proteins into a covalently linked dimer (Lu et al., 2006). Two dimers assemble into another dimer via noncovalent bonds forming a tetrameric unit. Experimental data of the structure of 3a are not yet available. Up to now, only computational models are generated (Hsu and Fischer, 2011; Krüger and Fischer, 2009). A variety of assembly protocols have been followed which can be categorized into protocols which screen the conformational space of the monomeric unit by a concerted movement of all TMDs and in those which build up the monomeric unit in a sequential manner. The latter means, two TMDs are assembled first following by the third TMD. Finally, in both protocols, the tetrameric assembly is done in a concerted screening protocol. While a concerted protocol proposes the third TMD to be pore lining (Krüger and Fischer, 2009), one of the sequential protocols (assembling TMD1 and TMD2 first followed by adding TMD3) proposes the second TMD to be pore lining in the tetramer (Hsu and Fischer, 2011). The rational for using the sequential assembly for the monomers is that it most likely resembles a biological relevant translocon based pathway of assembly. Along these investigations, the finding of unusual residues lining the lumen of the pore such as tyrosines and histidines is a common feature. In addition for TMD2 lining the pore, a ring of histidines is formed in the tetramer (Hsu and Fischer, 2011). With histidines pore lining, the channel is getting in line with M2 of influenza A and computational models of p7 from HCV (Patargias et al., 2006). It needs to be evaluated whether 3a is sensitive to protons. The role of 3a in the life cycle of SARS-CoV is not elucidated yet.

More recently, another open reading frame of SARS-CoV has been identified to exhibit channel activity. ORF 8 is separated into two ORFs 8a and 8b in human isolates with a 29-nt deletion (Guan et al., 2003). Protein 8a has been identified to amplify viral release and to induce the hyperpolarization of the mitochondrial membrane (Chen et al., 2007a). Consequently, it is concluded that 8a is involved in cellular apoptosis. Patients with antibodies against 8a recovered from SARS-CoV infection. 8a is identified as a 39 amino acid transmembrane protein (Guan et al., 2003). Secondary structure prediction programs suggest the N terminus to be transmembrane followed by an extramembrane domain containing approximately 15–20 (Chen et al., 2011). A peptide corresponding to full-length 8a derived from SPPS and reconstituted into artificial lipid membranes exhibits weak cation specific channel activity with conductance of around 9 pS at elevated temperatures (38.5 °C). Since the sequence of 8a is rich of cysteins, experiments have also been done under reducing conditions. Computational modeling of the TMD reveals a sequence of cysteins on one side parallel to the helix axis and a hydrophobic stretch of serines and threonines on the opposing side. Assembling the single TMD around a central axis into tetra-, penta-, and hexamers delivers potential structures for the putative pore. Consequent molecular dynamics simulations show a pentameric model maintaining a continuous water column. This model shows Ser-11 and Thr-8 as well as Cys-15 to be pore lining. In addition, the C terminal mouth is surrounded by Arg-22.

Summarizing the findings about SARS-CoV, with its large genome it seems that the virus hosts three potential channel-forming proteins, E, 3a, and 8a. All three of them are identified as auxiliary proteins, also interacting with a series of other viral and host proteins (Narayanan et al., 2008). All three proteins have in common, that their roles within the viral life cycle have yet to be identified. Channel activity is found either with expression of the protein in other cells or by reconstitution of the proteins into artificial lipid membranes. The question emerges why the virus needs three channels while all other channel expressing viruses known to date proteins only need one type of channel protein.

2.2.3. 2B from Entero viruses

Entero viruses among which poliovirus, coxsackie virus, and ECHO virus are listed encode a nonstructural 97–99 amino acid protein called 2B (Aldabe et al., 1996; Doedens and Kirkegaard, 1995; van Kuppeveld et al., 1995). It has been identified to render the membrane of the endoplasmic reticulum and the plasma membrane permeable for small molecules and especially calcium ions (Aldabe et al., 1996; Doedens and Kirkegaard, 1995; van Kuppeveld et al., 1997a). It has also been reported that 2B is retained in the Golgi apparatus where it increases the release of Ca ions, a role which is also found for the endoplasmic reticulum in the presence of 2B (de Jong

et al., 2006). More recently, it has been reported that 2B is also able to conduct monovalent ions and its conductance can be blocked by a known chloride channel blockers such as 4,4′-diisothiocyanatostilben-2,2′-disulfonic acid (Xie et al., 2011). The measurements have been done using two electrode voltage clamp conditions and with 2B expressed in *Xenopus* oocytes. 2B is composed of two hydrophobic domains (van Kuppeveld et al., 1995, 1997b) and is found to homooligomerize into tetramers (Cuconati et al., 1998; de Jong et al., 2002; van Kuppeveld et al., 2002). In a computational approach, a dimeric and tetrameric structure of 2B from Polio virus have been proposed (Patargias et al., 2009). The individual TMDs have been modeled into an ideal helix and inserted into a fully hydrated lipid bilayer to relax the structure during a short molecular dynamics simulation. The individual TMDs have then been taken to form the monomer. After another MD simulation, the tetramers have been produced and also relaxed for many nanoseconds of MD simulations. From those models, it is suggested that both TMDs contribute to form the lumen of the pore. It is further suggested that lysines contribute to the inner face of the pore. A short peptide based on 20 amino acids of the second TMD has been able to permeabilize the plasmamembrane of cells (Madan et al., 2007). The experiments show that TMD2 alone could form a pore and possibly is at least part of the pore lining motif of the bundle made of the full-length protein. For extended reviews, please consult Fischer and Krüger (2009) and Gonzales and Carrasco (2003).

2.2.4. Kcv from *Paramecium bursaria* chlorella virus

Plant viruses such as green algae infecting *P. bursaria* chlorella virus (PBCV-1; Yamada et al., 2006) express a 94 amino acid potassium selective channel, called Kcv (Gazzarrini et al., 2003; Plugge et al., 2000). Sequence homology with the potassium KcsA (Doyle et al., 1998) has been proposed and consequently a structural model is suggested to be similar to KcsA. In *Xenopus* oocytes, the protein induces channel activity and it is suggested that the channel is important for viral entry (Mehmel et al., 2003; Neupärtl et al., 2008). It can be blocked by amantadine and barium ions (Plugge et al., 2000). A series of mutants have been analyzed in respect to the consequences on the physiology of the channel and its mechanism of function (Gazzarrini et al., 2004). Extended physiological measurements reveal two types of kinetics of the channel (Abenavoli et al., 2009). This identifies that despite of the small size and without any extramembrane domains, the protein undergoes diverse gating behavior similar to other K^+ channels. Computational models of Kcv built on homology modeling and implementation of NMR spectroscopic data have been generated (Tayefeh et al., 2007, 2009). The simulations show functional relevant amino acids and facilitated ion movement through the selectivity filter. Another K^+ channel has also been found in the genome of brown algae infecting *Ectocarpus siliculosus* and called Kesv (Chen et al., 2005).

With its 124 amino acids, it is slightly longer than Kcv. Three potential hydrophobic regions have been identified by sequence analysis. The channel is blocked by barium ions and amantadine.

2.3. Remarks

Structural studies are most advanced for M2 and Vpu. Also topological information is available for p7. These studies on the structure of the channel deliver a snapshot of the overall dynamics the protein exhibits. Usually, special biochemical conditions are applied to grab the protein for structural studies or to trap the protein into a specific conformational state. The combination of the pictures allows assessment to the mechanics of the protein. Inevitable to these investigations is the use of computational tools to catch a glimpse about the dynamics on an atomistic scale.

Simulations on gating are widely applied to M2 to identify the roles of the histidines (Carnevale et al., 2010; Chen et al., 2007b; Khurana et al., 2009). In case of other VCPs, the studies are focusing on the generation of structural models (Fischer and Hsu, 2011).

3. Evaluation of the Mechanism of Function along Known Channel Proteins and Toxins

There are many questions linked with investigations on VCPs. Some of the VCPs form covalently linked dimmers which assemble into proton conducting tetramers for which gating is achieved by a ring of histidines. Other VCPs assemble into oligomers and it is anticipated that any hydrophilic residue within the TMD will point toward a putative pore (Vpu, E, 8a). These channels neither are covalently linked nor conduct protons. The question about what triggers a defined opening is unknown. To summarize the mechanics of the proteins are fully in the dark. For p7, it can be speculated that, with the suggestion of histidines facing a pore or being aligned at a helix–helix interface within the membrane, the protein is sensitive to the surrounding pH as well. In addition to that, histidines can interact with metal to stabilize the assembly. With the tritopic 3a forming covalently linked dimers which assemble into tetramers, speculations about more sophisticated gating mechanisms are allowed.

Reviewing the mechanism of function at this stage of research on viral channel-forming proteins is still very speculative due to a lack of structural details for most of the proteins. The accumulation of structural information for proton channel M2 and with it clues about its mechanics is definitively sparked by the fact that M2 has been very quickly identified as a target for antiviral therapy due to its importance in the viral life cycle (Hay et al., 1985).

It is also this circumstance which has ignited the hunt for channel proteins in other viruses and their potency to serve as antiviral target.

Evaluating potential mechanics of these proteins (Fig. 6.5), comparative investigations are the route to go at this stage. In doing so, the sequence of the TMDs of individual viral channels are compared with those of the host channels and toxins for which structural and more functional information are available (Fischer and Hsu, 2011; Schindler and Fischer, 2011). Based on sequence alignment of the TMDs of these proteins, speculation and links of how the viral proteins may work are given.

In the following, host channel proteins and toxins are chosen to be reviewed which have been identified to show sequence identity with the TMDs of selected viral channels such as Vpu, p7, 2B, and 3a (Fischer and Hsu, 2011; Schindler and Fischer, 2011). The introduction of the host channels and toxins follows a review of ideas about referring to the mechanics of the respective viral channels.

3.1. Pore forming toxins

Pore forming toxins (PFTs) are a class of proteins which are expressed by bacteria as well as higher organisms (Iacovache et al., 2008) and even human cells (Agerberth et al., 1995) to protect them against or support an attack. Their role is to punch holes into the membrane and enable the draining of the cytoplasmic interior and thereby leading to cell death. Pores formed by this class of proteins tend to be highly unselective. They are considered in this review since in a recent study about sequence alignment of Vpu from HIV-1 with ClyA identified an alignment of the TMD of Vpu with the membrane spanning domain of ClyA, αA (Fischer and Hsu, 2011). There are two classes of PFTs depending on the membrane spanning motif they use: those which adopt a helical motif, α-PFTs, such as ClyA (Mueller et al., 2009), and those which adopt a β-barrel motif, β-PFTs, such as α-hemolysin of *Staphylococcus aureus* (Song et al., 1996). (For an overview, refer to http://blanco.biomol.uci.edu/Membrane_Proteins_xtal.html.) The mode of action of PFTs goes through various steps. The proteins are released, they will "see" an aqueous environment, have to attach to the membrane, and assemble to finally convert into a membrane protein which intrudes into the membrane. Many of these modes are not comparable to the mode of action of Vpu except when the toxins are embedded in the membrane to form unselective pores.

ClyA belongs to the class of α-PFTs. In its functional form, it forms a 400 kDa pore of 12 monomers with a height of 13 nm and an inner pore diameter of 7 nm (Mueller et al., 2009). The single protein consists of four helices, αA, αB, αC, and αF which are oriented parallel to the membrane surface. Upon membrane attachment of the monomer, its β-tongue,

βt, named like that because of the short β-fold found in this region, initiates membrane anchoring and a rise of the monomer aligning the helices perpendicular to the membrane surface. At this stage, assembly is also initiated and the monomers align head-to-head into a dodecamer. Assembly facilitates the interlocking of the 12 αAs into an iris-like arrangement which intrudes into the membrane stabilizing the pore. Due to the enormous size, this pore can then be considered to be "open" leading to the vanishing of the hydrophobic permeation barrier of the lipid membrane and with it of any electrochemical or substrate gradients across the plasma membrane. Smaller PFTs such as alamethicin, magainin, or melittin follow the same strategy with the only difference that they form either a pore fully mantled by protein (barrel-stave model) or a pore with the phospholipid head groups part of the mantling wall (toroidal model) (Huang, 2000; Shai and Oren, 2001).

At this stage, there is no available information on a gating mechanism of the smaller PFTs unless due to thermal fluctuations within the membrane, consequent membrane curvature, and stress alterations the pore may collapse. This may not be the case for the larger PFTs such as ClyA or α-hemolysin. Due to the role of these proteins, any "sophistication" of the mechanics of gating would not be necessary anyway.

Due to the similarity of Vpu with αA of ClyA, the following speculations are allowed: Vpu assembles into homooligomers. Numbers range from 4 to 5 as minimal assembly units. With the tetramer, most likely no channel activity should be possible adopting a tight helix packing motif. With a pentameric assembly, ions would be able to pass through and with hexameric or larger bundles ion selectivity should be lost and substrates may also be able to pass through. With 5 and more monomers, the pore could be mantled by the TMDs. Tilts of the TMD of Vpu have been measured and range from about 6° (in DMPC; Kukol and Arkin, 1999) to 13° (Park et al., 2003), 18° (Park and Opella, 2005), and lower than 20° (Sharpe et al., 2006) with the latter three values obtained with peptide reconstituted into DOPC. Upon thinning of the membrane, the tilt of Vpu will increase because of compensating for the mismatch with the lipid bilayer (Park and Opella, 2005). The angles obtained for Vpu are lower than the observed tilt in the crystal structure of ClyA 2WCD (Mueller et al., 2009) which adopts values around 45° in detergents. It is possible that in a lipid bilayer this value may be lower as well. It is therefore speculated for Vpu that possibly lipid composition and lipid dynamics may act as trigger to gate the protein bundle (Mehnert et al., 2007, 2008) (Fig. 6.4).

Conductance values for Vpu are within a range of 30–60 pS (Schubert et al., 1996b) and exhibit gating into subconductance states (Ma et al., 2002; Mehnert et al., 2008). Nevertheless, these values rather indicate ion channel activity than "brute" conductance through a hole in the bilayer.

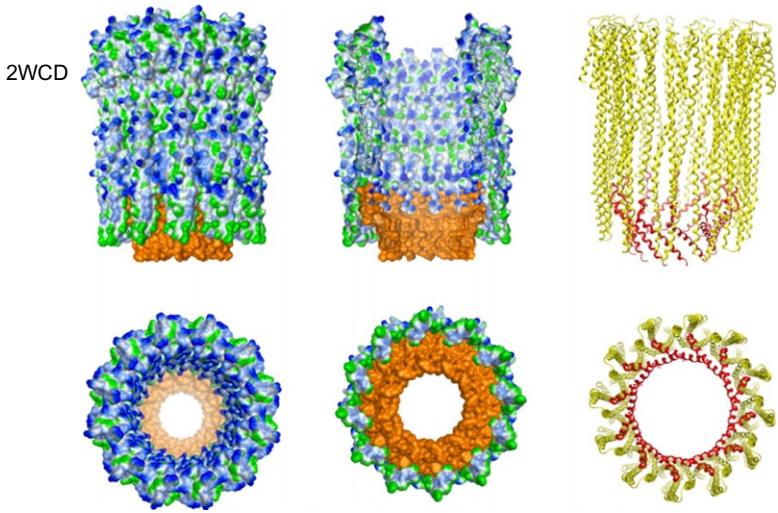

Figure 6.4 Crystal structure of toxin ClyA (2WCD) (Mueller et al., 2009). The structure is shown in "Gaussian Contact Mode" (MOE software) indicating hydrophilic residues in blue and hydrophobic residues in green. The membrane inserted segment αA, which shows sequence alignment with the TMD of Vpu, is either highlighted in orange or in red (Fischer and Hsu, 2011). Left: side view and below view from the extracellular side; middle: view inside the pore, omitting several units and below view from the cytoplasmic side; right: backbone representation of the protein in side view and cytoplasmic view below.

Concluding from the above, gating may be driven by stochastic events triggered by the thermodynamics of the environment (Fig. 6.5A and B). Assuming a "sliding mechanism" to rise the tilted TMDs (Krüger and Fischer, 2009), possibly in combination with minimal rotational movements, since the peptide is dynamic in the lipid bilayer (Park et al., 2006), it can easily be triggered by membrane thickening or thinning. A concerted rotation around each of the helix axis (Bour and Strebel, 2003; Montal, 2003) needs to cross large energy barriers (Krüger and Fischer, 2009) but would on the other hand be mostly independent of lipid thickness.

The overall number of monomers forming the pore is still a matter of debate since conflicting pore geometries and oligomeric states are proposed. The zipper motif (Kim et al., 2005) composed by a line of alanines, formed when adopting a helical conformation (Fischer, 2003), is an important tool for membrane protein packing. NMR spectroscopic data reveal a splitting of NMR signals especially for Ala-18 which is interpreted as that the

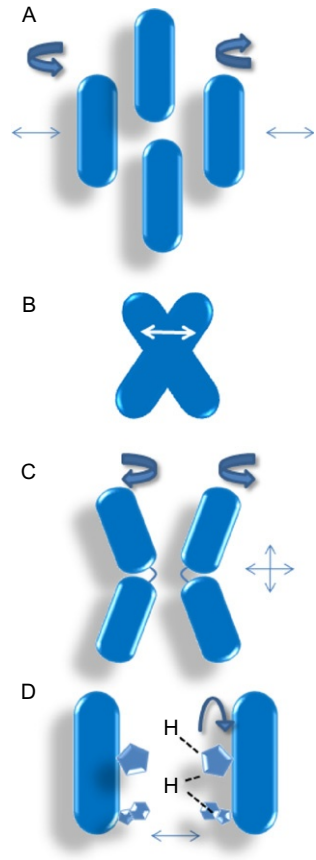

Figure 6.5 Potential conformational elements used in channel gating and discussed for viral channels. (A) Translational motion/diffusion of individual proteins and their TMDs including rotational motion; (B) tilt motion or TMDs sliding which increases the crossing angle; (D) rotational motion of kinked TMDs leading to a kind of "twisting" including lateral and/or vertical motion; (C) protonation of residues which includes rotational motion of the residue and a consequent bending and tilting of the TMDs.

splitting is caused by interhelix packing (Sharpe et al., 2006). This information has to be taken into account when assembling Vpu.

3.2. Potassium channels (KcsA)

With the emergence of the crystal structure (0.32 nm) of the bacterial (*Streptomyces lividans*) potassium channel KcsA, a keystone for ion channel structure has been delivered (Doyle et al., 1998; MacKinnon, 2003).

Its topology has been identified to be bitopic with an inner and outer helix. The two helices are linked by the "pore helix" and the selectivity filter. Four subunits form the channel by lining a pathway for ions to cross the bilayer. The passage of an ion can be described as passing a gate on the cytoplasmic side and moving into a vestibule which stabilizes the ion via the dipole moment of a so-called inner helix. The ions need to pass the selectivity filer in a concerted motion with already potassium ions located within the filter already. With its high selectivity, KcsA shows similarity with voltage-gated K channels (Kv) in terms of ion permeation and similarity in topology with inward rectifying K channels (Kir). Important to note is that KcsA channels are triggered by pH changes. Deciphering the cause of the enormous selectivity of K channels for potassium over sodium is a challenge up to date (Noskov and Roux, 2006). It is anticipated that the structure of KcsA represents a closed stage. With the structure (0.33 nm) of a prokaryotic (*Methanobacterium thermoautotrophicum*) calcium-gated K channel, a model in the open stage is described (Jiang et al., 2002a,b). With this discovery and in comparison with the KscA structure, a gating mechanism can be proposed (Sansom et al., 2002). During activation, the inner helices push radial outward and open the constriction at the cytoplasmic side. This opening is accompanied by a hinge around a glycine residue at position 99 (G99). This is the most pronounced conformational change so far described for ion channels. The selectivity filter remains unchanged in its structural position and the outer helix only undergoes marginal conformational changes (Jiang et al., 2002b). Also, hydrogen bonding seems to be essential for the gating mechanism (Rapedius et al., 2007). As a conclusion for the context of this review and in respect to the findings for Vpu in relation to KcsA (Fischer and Hsu, 2011), the four outer helices seem to fulfill the role as a sheltering corona toward the lipid environment.

Generation of computational models of a conducting pore is biased toward the idea, and findings in other channels, that hydrophilic residues have to face the lumen of a pore. Sequence identity of the TMD of Vpu is found with the outer helix of the K channel TASK (Hsu et al., 2004). It has been speculated that Vpu results from molecular piracy. Due to similarity with the outer helix of TASK, it could rather be interpreted that Vpu also mainly acts on the lipid membrane.

3.3. Mechanosensitive channels

Mechanosensitive channels (Msc) belong to a class of ion channels which respond on the mechanical stress within a lipid bilayer (Anishkin and Sukharev, 2009; Kloda et al., 2008; Perozo and Rees, 2003). They are designed by nature to sense alterations in osmotic and mechanic pressures imposed onto the lipid membrane. By sensing the change, they enable the physiological relevant ions to diffuse passively through their interior to alter

electrochemical and substrate gradients of relevant cells (Zhou et al., 1991). Consequently, these membrane proteins convert the mechanical stress into readable signals for our nervous system. Two types of Msc can be distinguished according to the levels of conductance they generate: mechanosensitive channels of small (MscS) and large conductance (MscL). For both types of channels, crystallographic data from bacterial channels are available (Bass et al., 2002; Chang et al., 1998; Liu et al., 2009; Steinbacher et al., 2007; Wang et al., 2008). Focusing on MscL and the crystal structure of a homologous protein from *Mycobacterium tuberculosis* (Chang et al., 1998), the protein has been identified to consist of a pentameric homoassembly with two TMDs. Its water filled pore is aligned with hydrophilic residues and has a diameter of about 1.8 nm. It is assumed that this structure catches the closed state of the channel. Other structures are reported to be due to intermediate states of the opening (Liu et al., 2009). This structure (Liu et al., 2009) includes a truncation in the cytoplasmic domain which allows the TMDs to adopt an increased tilt compared to the "closed" and stable state of the protein. This protein has shown increased current and therefore supports the idea of now having a structure in a more open state, albeit the still very narrow pore diameter. However, the protein is reported to be a tetramer in contrast to the earlier studies of the MscL in the closed state (Chang et al., 1998). Nevertheless, the larger tilt of the TMDs in a partially open state compared to the tilt in the closed structure indicates a sliding mechanism for opening (Fig. 6.5B).

Interesting to note is that similar to p7, over time, and with different experiments, several oligomeric states have been proposed. Biochemical data (Sukharev et al., 1999) and two-dimensional crystallography (Saint et al., 1998) support the formation of hexameric assemblies of the protein. The crystallographic data identify pentameric (Chang et al., 1998) and tetrameric structures (Liu et al., 2009). It is up to further investigations to decide about the implications of the findings on the mechanism of function of this channel protein.

Proteins p7 and 2B align particularly good with the TMDs of the mechanosensitive channel MscL (Schindler and Fischer, 2011). This ignites a discussion of whether the two proteins would also respond to mechanical stress profiles of the lipid bilayer and gate in a similar way (Fig. 6.5B).

3.4. Ligand-gated ion channels: nAChR, ELIC, GLIC

The nAChR is part of the cystein-loop receptor super family of pentameric neurotransmitter-gated ion channels (Le Novère and Changeux, 1995) triggered by acetylcholine and susceptible to nicotine. The channel protein assembles symmetrically around a fivefold central axis. Within the family, the channel can exist in homo- and heteromeric assemblies of about 290 kDa (Unwin, 2005). Upon acetylcholine binding, the channel converts into

an open state enabling a flux of mostly monovalent cations across the lipid membrane. With its location at nerve-muscle synapses, its action induces fast chemical transmission of nerve signals.

Information about the morphology of the protein has mostly been derived from electron microscopy (Unwin, 2003, 2005; Unwin et al., 1988). The channel can be divided into three parts, a large extracellular domain hosting the N termini of the subunits, a membrane spanning part which contains the gate, and a smaller cytoplasmic domain. The overall length of the protein is 16 nm, with a pore of about 2 nm in diameter. The two binding sites of the neurotransmitter are about 4 nm above the membrane surface and opposing each other. Cryo-electron microscopy has been used to derive structural features of the receptor when briefly exposed to acetylcholine and immediately frozen (Unwin, 1995, 1998). The data yield a resolution of 0.9 nm. In comparison with earlier structures, which are related to the closed state, the major changes in the open state are due to an alteration of the ligand binding domain which initiates a small axial rotation in each of the two TMDs of the respective subunits almost 5 nm away. Imposing structural data into the models suggest that the closed state is due to a constriction of the pore in the middle of the membrane caused by Leu-251 from each subunit, so to speak a ring of leucines. The residues are part of the pore lining M2 helix of each subunit. The constriction does not result from an almost overlap of the five residues; it rather follows from an approach of these residues. The consequence of this approach is a hydrophobic barrier which interrupts the water column which would otherwise fit through the pore. Upon activation, the ring widens through a rotational motion, twist-to-open (Miyazawa et al., 2003; Unwin, 2003), giving enough space so water can pass this barrier, which represents the gate of the channel. Passing of water in the open stage has been shown using molecular dynamics simulations on the TMDs of the receptor embedded in a hydrated lipid bilayer (Beckstein and Sansom, 2006). It has been suggested that this mechanism is a blue print for other members of the ligand-gated ion channels (Unwin, 2003).

The bacterium *Erwinia chrysanthemi* also expresses a ligand-gated ion channel which belongs to the family of pentameric ligand-gated ion channels (ELIC). Crystal structures of this channel in its potential closed state have been obtained (Hilf and Dutzler, 2008). The ELIC channels show 16% sequence homology with nAChRα and comprise the closest to a structure representing this class of ligand-gated ion channels. In terms of the extramembrane and transmembrane part, this channel approximately adopts the same dimensions (9.5×11 nm) as the nAChR. In contrast to the nAChR, the channel has no cytoplasmic domain. The 10 β-strands of each of the subuntis mantle a cylindrical vestibule of approximately 1.6 nm diameter. Within the membrane, the pore narrows down to a diameter of 0.7 nm lined by one of four helical TMDs per subunit. Toward the

extramembranes segment, the transmembrane passage is confined by a ring of phenylalanines (F246) and leucines (L239). It is anticipated that these two constriction sites form a gate similar to the ring of leucines in the nAChR. Similar to the nAChR, the respective TMDs α1 and α3 are involved in inter-subunit contact, whereas α2 lines the pore. The TMD α4 is positioned at the periphery of the transmembrane subunit. Since the ligand triggering of the channel is not known, a study about the potential open state cannot be conducted. Cyanobacterium *Gloebacter violaceus* encodes a pentameric ion channel (GLIC) (Hilf and Dutzler, 2009) homologous to ELIC which is activated by low pH and does not desensitize after activation. Crystal structure of the channel at pH 4 with a resolution of 0.31 nm is therefore considered to show the open state of this channel. The structure of GLIC is "very similar" to the structure of ELIC and therefore the data are taken to identify a novel gating mechanism for the pentameric ligand-gated ion channels. The lumen of the pore in the transmembrane region confines gradually toward the cytoplasmic side. This is due to α2 and α3 helices which are rotated as a rigid unit around Val-267 by about 9°. The extramembrane part of the pore is flanked by hydrophobic residues while the cytoplasmic part is flanked by polar side chains. Both ends of the channel are guarded by rings of acidic residues. The narrow part at the cytoplasmic end is due to a ring of glutamate residues (E221). Crystallization of a mutant channel in which the glutamate residues are replaced by alanine under the same experimental conditions (low pH) reveals a similar overall conformation of the protein backbone but with the restriction derived from the glutamic acids being removed. This indicates that the local change of the amino acid residues does not alter their conformation and that only minor changes of the side chains allow an increased pore radius. The conclusion is that the glutamates interact directly with the permeant cations. The studies on both ELIC and GLIC are considered as studies on a closed (ELIC) and open (GLIC) ligand-gated ion channel. The opening is shown to result from a change in the tilt of two of the TMDs, α2 and α3, of each of the subunits around a pivot point two-third across the transmembrane pore. This is proposed for nAChR in contrast to the rotational motion of M2, which is similar to α2.

Protein 3a identifies identity with ligand-gated channels such as the nAChR and pGLIC/ELIC (Schindler and Fischer, 2011). This finding proposes that this large viral channel could be triggered by a ligand and also allows more complex gating behavior (Fig. 6.5A and C) for viral monotopic proteins such as Vpu, E protein, or 8a.

There is no identity with the pore lining part of the two types of toxins, such as the helical toxin ClyA and the β sheet structured α-hemolysin.

3.5. Proton conducting pumps and channels (bR, Hv1)

With M2 and BM2 proteins of influenza A and B, respectively, known to conduct protons, it is tempting to compare the mechanism of function of these proteins with other known proton conducting or transporting membrane proteins. One of the proteins, which allow protons to move across the membrane, is the light driven proton pump bacteriorhodopsin (bR) from *Halobacterium halobium* (Oesterhelt and Stoeckenius, 1971). Bacteriohodopsin is part of a family of light activated membrane proteins such as halorhodopsin and rhodospin. Albeit the fact that this protein needs light to activate a vectorial proton transport to build up a proton motif force, the movement of the protons along certain amino acids within the protein can give an idea of what is necessary for proton translocation. Bacteriorhodopsin has been analyzed in great details using techniques like cryo-electron microscopy (Henderson et al., 1990), FTIR spectroscopy (Rödig et al., 1999; Rothschild, 1992), NMR spectroscopy (Herzfeld and Lansing, 2002), X-ray crystallography (Edman et al., 1999), kinetic analysis (Kötting and Gerwert, 2005), and other techniques.

Describing its mechanism in short, the proton translocation mechanism is triggered by light leading to an isomerization of a retinal linked via a Schiff base to Lys-216 from its all *trans* into 13-*cis* conformation. This very fast event is followed by structural rearrangements of the protein which are characterized by specific spectral changes known as the photocycle of bR (Neutze et al., 2002). Structural rearrangements include kinks in two of the helices (C and F). Further, the action of localized water molecules (Fischer et al., 1994) in combination with a series of well-aligned titratable amino acids are necessary to achieve vectorial Grotthuss-type proton transport.

Another highly selective human voltage-gated proton channel is Hv1 (DeCoursey, 2008). Hv1 is polytopic membrane protein with four TMDs (Ramsey et al., 2010). Pore lining residues are also identified to be titratable ones. However, if these titratable residues are mutated, proton conductivity is not fully abrogated. Computational modeling studies using homologous models of voltage dependent potassium channels reveal that the structure allows water molecules within the pore of the channel. Combining the experimental and computational data, it is suggested that a water-wire exists to transfer the proton as selectively as this channel does, but that proton translocation does not necessarily require titratable residues.

What is the mechanism of function of M2, a proton channel of minimal design (Fig. 6.5D)? In comparison to other proton translocating and channeling proteins, it is missing a sequence of titratable residues within the pore. Localized and structurally defined water molecules are not yet reported. This may be due to the fact that a structure of full-length M2 protein is not yet at hand. The gating mechanism may find some relation to bR in as much the histidines of M2 rotate or "flip," similar to *cis/trans*

isomerization in bR, and "shuffle" the proton to the cytoplasmic side to be picked up by Trp-41 and Asp-44. Structural changes for M2 seem to involve a change of the overall tilt of the protein assembly. Similarities are thus far speculative and it remains the question in how far the design of M2 resembles a novel structural concept of proton translocation.

3.6. The role of lipids

Most of the VCPs are smaller in size than their host channels. With about 100 amino acids in length, they harbor a maximum of two TMDs. Only 3a from SARS-CoV harbors three domains but is with 274 amino acids almost three times as long. With one or two TMDs per protein which itself needs to self-assemble to form a channel, it is anticipated that the channel should be sensitive to the lipid environment, which is mentioned for Vpu (Mehnert et al., 2008). Additional TMDs per protein, as found in many other host channels, could act as a "mechanical buffer" toward the lipid membrane. Functional information is mainly done either with the proteins reconstituted into artificial lipid compositions or with the protein expressed in *Xenopus* oocytes (Table 6.1). Structural data from NMR or X-ray sources are also recorded in artificial environments.

There is emerging evidence that lipid rafts are playing a highly important role in the cellular life cycle of enveloped viruses (Brügger et al., 2006; Campbell et al., 2001). Lipid rafts are cholesterol and glycosphingolipid rich detergent-resistant membrane patches (Simons and Ikonen, 1997; Stier and Sackmann, 1973). Purification of M2 from infected cells or eukaryotic expression systems has identified the presence of cholesterol (Schroeder, 2010; Schroeder et al., 2005). Therefore, it has been suggested that M2 from influenza A is attached to lipid rafts *in vivo* (Lin and Schroeder, 2001; Schroeder and Lin, 2005). Since all of the M2 channel recording data identify the function of M2, even when taking just its TMD and not even covalently linked together, it seems that rafts just only serve as a scaffold for *in vivo* function. To combine these findings, it is suggested that in the case of a raft attachment of a monomeric protein, or dimeric protein in case of M2, several of the raft patches can form a trapped cholesterol free "patch" in which the protein can function as a proton channel (Lin and Schroeder, 2001).

Raft association has also been reported for Vpu (Ruiz et al., 2010b). Expression of Vpu in human 293 cell lines reveals that it partitioned into detergent-resistant membrane microdomains. Its partitioning could be abolished when residues in the TMD are substituted by alanines. Mutations of Trp22 and a sequence on the middle of the domain, IVV19, are key residues responsible for microdomain integration. Taken together with computational modeling data in which it is suggested that Vpu is flexible and adopts to its environment via residues in the region from Ile-17 to Ser-24 (Krüger and Fischer, 2008; Park et al., 2003), replacement of these

Table 6.1 Overview of structural and functional aspects of the viral channel proteins

	Virus	Length	TMDs	Functional units	Selectivity	Substituted	Type	Solution NMR structures	Solid state NMR	X-ray structure	EM	Reported drugs	Interacting proteins or lipids
M2	Influenza A	97	1	Tetramer (covalently linked dimer of a dimer)	H^+	Some subtypes palmitylated	III	2KWX, 2RLF, 2KIH (S31N)	2KAD, 1MP6, 2KQT, 2H95, 2L0J, 1NYJ	3LBW (1.65 Å), 3BKD (2.05 Å), 3C9J (3.05 Å)		Amantadine, rimantadine, Spiropiperidine	Rafts
PB1-F2	Influenza A	Appr. 90	1	Oligomers	None-selective			2HN8					
BM2	Influenza B	109	1	Tetramer	H^+	Phosphorylated	III	2KIX, 2KJ1					
Vpu	HIV-1	81	1	Most likely pentamer, tetramer suggested	Weak cation selective	Phosphorylated	I	2JPX, 2GOF, 2GOH, 1VPU[C], 2K7Y[C], 1WBR[C]	1PJE, 1PI7, 1PI8			Hexamethylene amiloride, Substituted naphtoyl guanidines	$CD4^h$, $CD74^h$, $CD317^h$, BST-2/ $Tetherin^h$, rafts
E	SARS-CoV	76	1	Pentamer								Hexamethylene amiloride	Rafts
8a	SARS-CoV	39	1	Pentamer suggested	Weak cation selective								
6K	Alphavirus	60	1	Larger oligomers	Cation selective	Palmitylated							p62/E1
P7	Hepatitis C	63	2	Hexamer, heptamer reported	Weak cation selective		C and N term. to ER lumen	2K8J (TMD2)			Luik et al. (2009), Clarke et al. (2006), Griffin et al. (2003)	Substituted naphtoyl guanidines, hexamethylene amiloride, amantadine	E2, NS2
6K	Alpha virus	Appr. 60	2		Large conductance	Palmitylated							
2B	Enterovirus	97–99	2	Tetramer	Ca^{2+} conductance, small molecules							4,4′-diisothiocyanatostilben-2,2′-disulfonic acid	
Kcv	PBVC-1	94	2	Tetramer	K^+							Amantadine	
3a	SARS-CoV	274	3	Tetramer	Cation selective							Emodin	Rafts

The code for structural information refers to the four letter code used by the RCSB protein data bank (www.pdb.org). C, cytoplasmic domain. For the X-ray structures the resolution is given in Å.

residues hampers essential flexibility necessary for domain integration. Important to note is that raft association is not required for CD4 down-regulation and that the above mutations can be correlated with a reduced particle release (Ruiz et al., 2010b). The exact placement within the microdomain is unclear and it could still be suggested, similar to M2, that channel activity of Vpu, which is independent of the cholesterol or sphingolipid content, could be achieved with the protein "released" from the raft into the confined space of an entrapped cholesterol free patch surrounded by rafts.

3a has been detected in membranous structures from expressing and infected cells (Huang et al., 2006). Membrane flotation essay identified 3a at relevant gradients indicating that the protein is associated with lipid membranes. When the membranous structures are treated with "raft" detergents, membrane floatation essay unravels that still some fraction of 3a is bound to membranes. It is therefore concluded that some of the 3a proteins are located within or at raft-like domains.

Additionally, E protein from SARS-Co has been identified to be located in lipid rafts expressed in HeLa cells as well (Liao et al., 2006).

The role of lipid composition on the mechanism of function of these channels is still little explored. With the channel proteins being raft associated, novel routes for antiviral therapy can be envisioned as discussed below (Ruiz et al., 2010b).

4. Interfering with Gating and Mode of Action

When blocking enzymes, the site of interference is well defined. The prime target site is the active region of the enzyme and eventually the outer side of the protein for, noncompetitive modulators. Membrane proteins contribute in drug therapy as drug targets to a large extent. For these proteins, the sites of interference are similar to enzymes. They are, for example, the docking sites of the biological ligand relevant for the receptor or ion channel. In cases of the latter, physical blocking of the channel, like a plough, is another option. For the extramembrane parts of the membrane proteins, other allosteric sites are equally important to be targeted by modulators.

Anticipating VCPs as targets, one can imagine that with their small size the lipid membrane plays an important role in the mechanism of function of these channels. The interaction of proteins with each other is also highly dependent on the dynamics of the lipid membrane (Langosch and Arkin, 2009). In other words, a potential drug does not necessarily need to interact with the protein but can also alter lipid dynamics which in turn

modulates protein function. Consequently, targeting, for example, lipid rafts could also have potential antiviral effects.

For some of the channel proteins, it emerges that they are interacting with a series of host factors via protein–protein interactions. The interaction is not confined to the extramembrane parts of the viral protein but also includes the TMDs. This is especially the case for Vpu and its interaction with the host factor BST-2. Hampering with protein–protein interaction is consequently a promising path for drug development.

Small molecule design is the way how man is trying to steer proteins for the cure of diseases. Viruses do not use small molecules, they rather create their own proteins to interfere with the mechanism of function of the host proteins. This concept inspires the development of drugs based on specific peptide–peptide interaction, such as peptide drugs.

4.1. Peptide drugs

The idea of a peptide drugs is to mimic the fold of the viral "protein ligand" which targets the host protein. The consequent blocking of the "protein ligand" interrupts the pathway of the viral protein within the cellular life cycle. The "coating" of the protein with peptides could either involve coating of the host or the viral protein. Potential peptide candidates as "coats" can be designed specifically by analyzing protein mechanics of both host and viral protein. Another option would be to search related proteins from data banks of phylomers®, proteins/peptides known to interrupt protein–protein interactions and used for protein silencing to validate targets (Watt et al., 2006). An example of such an approach which has been done for HIV-protease (Park, 2000) and HIV-integrase (Maroun et al., 2001; Zhao et al., 2003) indicates that this approach is a valid one for globular proteins.

Up to now, peptide drugs are used in a limited number of cases (Rishabh et al., 2009). However, their potential use is hypothesized to increase in the near future. Most striking is their highly specific mode of action which is expected to require a low dose to be administered. In addition, peptide drugs seem to be toxicologically safe and are found to exhibit lower side effects than their small molecule counterparts (Agyei and Danquah, 2011). Peptide drugs, despite the benefit, harbor some draw backs. Even though they are now more comfortably manufactured, administering of the drugs is still a major hurdle for their use on a broader scale (Shaji and Patole, 2008). Injection still is the major route for entering the drug into the body and up to now mostly used for treating diabetes. Among the routes of administering, oral or nasal routes are still the most favorable ones. Once administered, they also face difficulties such as fast enzymatic degradation, membrane impermeability due to their size, and metabolic stability. Thus, chemical modifications are also necessary not only to generate a deliverable form of the drug but also to increase the retention time of the drugs in the body to

improve their therapeutic value. One of the routes to improve the therapeutic value is to use peptides and develop peptidomimetics. The latter step is used to develop antimicrobial peptides (Godballe et al., 2011; Scott et al., 2008).

One of the first peptide like drugs proposed for antiviral therapy against membrane proteins, called 5-helix, has targeted gp41 from HIV-1, (Root et al., 2001). The idea of this peptide is to mimic the trimer-of-hairpins state of gp41 which consists of six helical elements of gp41 tightly packed. With only five helices, it is anticipated that the steric vacancy for the 6th helix will be taken up by the C-peptide region of the viral gp41 protein under native conditions. This interaction hampers the fold of gp41 into the trimer-of-hairpin state. Shorter peptides have been suggested to target the C terminal region further (Eckert and Kim, 2001). Also, conserved hydrophobic pockets in the N terminal region of gp41 are targeted by peptides including small molecules (Debnath, 2006). Currently, computational methods such as MD simulations have been applied to assess the binding and search for novel peptides (Strockbine and Rizzo, 2007). These developments have led to the first antifusion drug enfuvirtide (Poveda et al., 2005; Steffen and Pöhlmann, 2010). D-peptides, which show better affinity and bioavailability, are also reported to interfere with gp41 (Welch et al., 2007). Most recently, a peptide based on α_1-antitrypsin has shown promising results in patients (Forssmann et al., 2010). This 20-amino-acid peptide targets the fusion peptide of gp41.

Another strategy is to use peptides as a "molecular shield" of the host protein to protect it against interaction with viral proteins (Strangler et al., 2007). This concept is introduced with studies on preventing membrane associated Nef protein from HIV-1 to interact with the cellular transduction protein hemato-poietic-cell kinase (Hck). An artificial 12 amino acid proline-rich peptide abolishes the interaction between these two proteins.

4.2. Amantadine and derivatives

Amantadine (1-aminoadamantan) (Davies et al., 1964) and its derivatives have been used as one of the first antiviral drugs targeting M2, from influenza (Hay et al., 1985) (Fig. 6.6). Activity occurs in two stages. In a nonspecific way at higher concentrations (>0.1 mM), it affects the fusion event hampering the conformation of hemagglutinin to the fusion relevant conformational state. At a later stage of the viral life cycle and at much lower concentrations (0.1–5 μM), the drug acts strain specific against virus assembly. At this stage, it prevents the transformation of the fusion protein to forming a so-called high pH conformational stage. The nonspecific action can also be achieved by a series of amines (Hay et al., 1985). Mutant escape studies have shown that a series of hydrophobic residues at positions 27, 30, 31, and 34 of M2 (Hay et al., 1985) as well as 26 (Wang et al., 1993) are mutated in respective strains. Mapping the residues onto a helical wheel

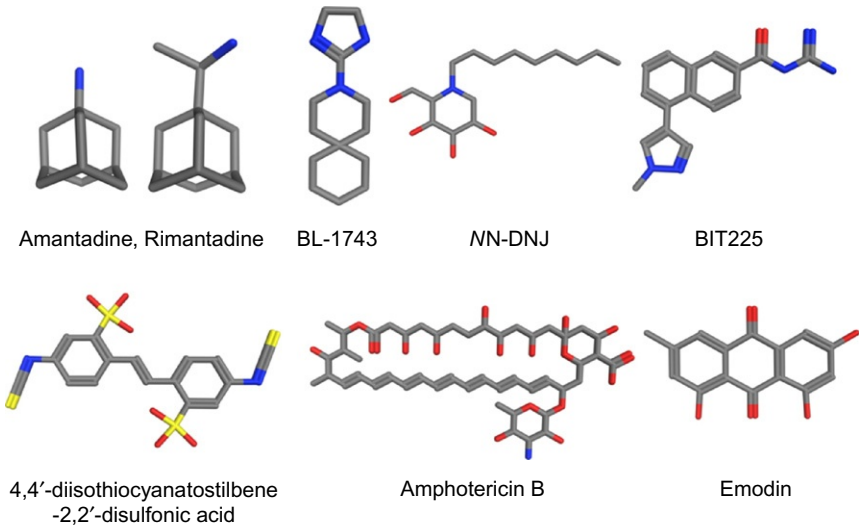

Figure 6.6 Potential drugs targeting VCPs. The drugs are shown in a stick modus following the CPK (Corey-Pauling-Koltun) color code: C in gray, nitrogen in blue, oxygen in red, and sulfur in yellow. Hydrogen atoms are not shown.

indicates that they are clustered on one side and assumed to face the inside of the bundle rather than the lipid environment (Sugrue and Hay, 1991). Thus, amantadine is assumed to intrude into the pore and block the protein by occlusion of the pore. Computational modeling of the drug in the center of an *in silico* model of the pore have been undertaken along this line (Sansom and Kerr, 1993). The M2 model has been built by copy-rotation of the monomer so that the hydrophilic residues face the lumen of the pore resulting in a slightly wider pore at the N terminal side than on the C terminal side. By positioning amantadine along the center of the pore and calculating for each position the interaction energy, a profile has been generated, which indicates a favorable binding site at the level of Ser-31 with the amantadine cube facing the N terminal mouth and the amino group the C terminal side. The same experiments with a cyclic-pentylamine have not revealed a favorable binding site at the same position. Neutron diffraction experiments confirmed a position in the area between Val-27 and Ser-31 (Duff et al., 1994). In a similar approach, using molecular dynamics simulations, amantadine has been positioned in the same way as reported (Sansom and Kerr, 1993) within the pore of M2 (Yi et al., 2008). The computational model of M2 has been leaned on an assembly based on NMR spectroscopic investigations (Hu et al., 2007). During the molecular dynamics simulation of 15 ns, the drug remains at its position around Ser-31 supporting the site of interaction of amantadine with M2. In

another proposal, amantadine is modeled to be within the central cavity with the amino group closer to the ring of histidines (Gandhi et al., 1999).

The proposal that the amino group is pointing toward the histidines from various sites within the N terminal side of the pore is verified by crystallographic studies (Stouffer et al., 2008). In this crystallographic study with a peptide corresponding to the TMD of M2 with only one mutation at position 34, where glycine is replaced by alanine, the location of amantadine is in the lumen of the pore on the N terminal side (3C9J; Stouffer et al. 2008). The crystal structure is obtained at low pH (pH 5.3) representing an open-like or conducting channel. Residues such as Val-27, Ala-30, Ser-31, and Gly-34 "trap" the drug so that its amino group points toward the C terminal side. It has been shown that mutation of these residues makes the channel insensitive to amantadine (Deyde et al., 2007). Since amantadine shows no cooperativity (Wang et al., 1993), this binding site is seen as the single site and the mode of action as an "occluding the pore." Based on solid state NMR spectroscopic studies of a peptide corresponding to the TMD of M2 derived from SPPS and reconstituted into DLPC (1,2-dilauroyl-sn-glycero-3-phosphatidylcholine), a binding site near Ser-31 has been suggested (Cady et al., 2009), which has been confirmed in a later experiment (Cady et al., 2010). Also, at higher amatadine concentrations, solid state NMR experiments suggest a second site at the C terminal side which should be considered as a weak binding site with low affinity (Cady et al., 2010). Molecular dynamics simulations over 15 ns with the amantadine bound M2 model from crystallography show that the drug remains at the position disrupting the continuous water column similar to the ring of valines (at position 27). Therefore, it is concluded that the mode of amantadine blocking is by interfering with the water molecules at the mouth of the pore.

In a solution, NMR spectroscopic investigation of a M2 peptide fusion construct corresponding to the TMD of the protein, which is reconstituted into DHPC (1,2-diheptanoyl-*sn*-glycero-3-phosphocholine), the amantadine derivative rimantadine has been detected to bind at the outside of the bundle at the C terminal side (Schnell and Chou, 2008). The experiments have been performed at pH of 7.5 which implies that the structural model represents a "closed" or non-active state of the protein. Rimantadine has a larger portioning coefficient between octanol and water than amantadine (Belshe et al., 1989) and possibly diffuses from the site of the membrane toward the protein. However, in this experiment four rimantadines per bundle are reported. Visualization of the binding site reveals that rimantadine sits within a pocket of hydrophobic residues Ile-42, Leu-40, and Leu-43 at the helix–helix interface. A blocking mechanism is suggested in which the drug is hampering the transition of the bundle into the open or H^+ gating state.

Based on these studies and earlier suggestions (Pinto and Lamb, 1995), it is reasonable to conclude that there are allosteric effects (Schnell and Chou, 2008) involved in the binding of amantadine derivatives to M2.

The mode of action for all drugs possibly involves an alteration of protein dynamics and based on the type of drug allosteric interactions rather than single-site blocking.

Amantadine is not reported to be active against BM2 (Paterson et al., 2003).

Amantadine has been reported to block p7 when the protein is expressed in *E. coli*, purified and reconstituted into lipid bilayers (Griffin et al., 2003). The protein, a His-p7 construct, shows burst activities at a holding potential of −120 mV. Adding amantadine to a final concentration of 1 μM into both chambers of the setup leads to a complete abrogation of the bursts after about 10 s. Application of amantadine to HCV replication cell cultures (Lohmann et al., 1999) revealed no effect of the drug on RNA replication, virus release, and infectivity of the virions (Steinmann et al., 2007b). Using a peptide derived from SPPS, corresponding to specific strain of HCV (GT 1a, isolate H77) which also is reconstituted into artificial lipid bilayer, addition of more than 10.3 μg/ml of amantadine has been necessary to affect channel activity of the p7 peptide. A full blocking, showing a zero channel activity, could not be achieved. A docking approach using AUTODOC 3.0 has been used to dock amantadine onto a computationally derived hexameric model of p7 (Patargias et al., 2006). The study proposes a binding site of the drug within the lumen of the pore between residues H17 and Ser21, with the amino group facing Ser21. The binding constant has been estimated to be around $K_i = 68$ μM. Since amantadine is located toward two monomers, it allows plenty of space for ions to pass the pore. So far, amantadine has shown little effect in clinical trials (Deltenre et al., 2004; Maynard et al., 2006). Currently, a series of derivatives of amantadine have been tested (Foster et al., 2011).

Channel activity of a peptide corresponding the N terminus of Vpu including the TMD, Vpu_{1-32}, derived from SPPS, reconstituted into artificial lipid bilayers is not affected by amantadine (Ewart et al., 2002).

Amantadine has also been reported to block Kcv (Plugge et al., 2000).

4.3. Spiropiperidine

Due to the emerging resistance of influenza strains against amantadines and derivatives and also due to the side effects caused in the central nervous system of the latter compounds, a novel class of drugs, spiropiperidines, is currently investigated (Wang et al., 2009a) (BL-1743, Fig. 6.6). Solid state NMR studies reveal that the derivative 3-azaspiro[5.5]undecane hydrochloride alters the dynamics of the protein and affects a larger series of amino residues within the pore. Using a docking approach (Autodock) with the drug bound crystal structure of M2 (3C9J (Stouffer et al., 2008), a binding site similar to amantadine is proposed.

4.4. Iminosugars

Iminosugars are more effective than amantadine against p7, as indicated by channel recordings measurements which is also confirmed by cell based essays (Steinmann et al., 2007b). Especially, long alkyl chain iminosugars block p7 much stronger than iminosugars with short alkyl chains.

4.5. Hexamethylene amiloride and derivatives

It has been reported that Vpu is sensitive to derivatives of amiloride (Ewart et al., 2002). Experiments have been done with Vpu expressed in HeLa cells together with the Gag protein of HIV-1. Budding virus like particles have been observed by electron microscopy. Experiments in the presence of HMA in the culture medium after transfection of the cells with the expression plasmid lead to an almost complete inhibition of the budding process. Channel recording of a recombinant Vpu protein, expressed in *E. coli*, could be blocked with the addition of HMA in a range of 25–125 μM. An allosteric blocking could be anticipated since it is reported that at lower HMA concentrations blockage is not complete. Blocking has also been dependent of the applied potential. Therefore, it seems that blocking also depends on the side of which the drug approaches the channel. In the same type of experiments, a derivative dimethyl amiloride (DMA) also affects channel recordings in a similar way. Since blocking by DMA has been less complete than by HMA at higher concentrations, a lower potency for DMA has been concluded. Amiloride itself has shown no effect in this study. The data have been confirmed in a study using a Vpu peptide (Vpu_{1-32}) reconstituted into artificial "micro" bilayers which are spanning a porous *silicon* device (Römer et al., 2004). Adding 100 μM of both HMA and DMA to a measurement setup results in a full blocking of channel activity, while amiloride does not show any effect on the activity. In a computational study with a helical model of the monomeric TMD of Vpu and in an assembly of five and six TMDs forming bundles, putative binding sites of HMA and amiloride have been evaluated (Kim et al., 2006). Most striking are calculations of an estimated free energy using the docking program AUTODOCK 3.0. The calculations reveal lowest binding constant for HMA interacting with the pentameric bundle. Binding sites of HMA within the bundle identify an interaction of the guanidinium group of HMA at the site of Ser-24. Interaction of HMA with a monomeric TMD identifies Trp-23 as a potential site for interactions, suggesting π–π interactions. The computational data support the currently emerging idea of multiple binding sites of antiviral channel drugs and with it the suggestion of allosteric binding modes (Pielak et al., 2009; Schnell and Chou, 2008). From investigations on Vpu interacting with HMA—two different inhibition levels at various drug concentrations in bilayer recording studies and

two putative binding sites identified in a docking approach—it seems very likely that Vpu also follows this path.

HMA is reported to block channel activity of full-length p7 when derived from SPPS, purified and reconstituted into artificial lipid bilayers (Premkumar et al., 2004). In repeatedly, recorded experiments HMA has been added to the *cis* side of a bilayer recording setup which contained 500 mM KCl while the *trans* side contains 10 times less KCl.

4.6. Substituted naphtoyl guanidines

To date, *N*-[5-(1-methyl-1*H*-pyrazol-4-yl)-naphtalene-2-carbonyl]-guanidine (BIT225, Fig. 6.6) is the second most advanced class of antiviral drugs targeting a VCP. Synthetic p7 derived from SPPS and reconstituted into lipid bilayers can be blocked by BIT225 at a concentration of 100 μM BIT225 on both sides of the measurement chamber and both filled with 50 mM KCl (Luscombe et al., 2010). An IC_{50} in the submicromolar range has been reported with a cell-based essay system using the model virus BVDV (bovine viral diarrhea virus). In combination with interferon alpha-2b, (rIFNα-2b) even a synergistic affect has been observed. BIT225 has now successfully completed phase Ib/IIa trials. The drug is also evaluated for its affection of Vpu (Khoury et al., 2010). A synthetic peptide construct representing the first 32 amino acids of Vpu including the TMD ($Vpu_{1–32}$), reconstituted into lipid bilayers shows channel activity which is knocked out by a 40 μM solution of BIT225. In monocyte-derived macrophages chronically infected with HIV-2, which does not encode Vpu, no affect has been observed, which supports that Vpu is the target. A wide range of HIV-1 isolates are susceptible to BIT225 as well. Based on a computational evaluation of several guanidines on a pentameric $Vpu_{1–32}$, BIT225 has come out as a highly potential candidate (Patargias et al., 2010). The study uses models of Vpu TMDs in which the serines (Ser-24) are facing the potential lumen of the pore. For this investigation, the docking software FlexX (BiosolvIT) has been used.

4.7. Diisothiocyanatostilbens

The small molecule 4,4′-diisothiocyanatostilben-2,2′-disulfonic acid has been reported to block 2B (Xie et al., 2011).

4.8. Amphotericin B methyl ester

Amphotericin B methyl ester (AME) is a water soluble derivative of amphotericin B (Waheed et al., 2008) (Fig. 6.6). It is water soluble, shows low toxicity, and is able to bind to cholesterol within the membrane. Viral membranes, especially those in HIV-1 virions, are found to exhibit some

similarity in the composition to lipid rafts (Aloia et al., 1993; Brügger et al., 2006). With the rafts containing cholesterol, AME alters the properties of the viral membrane. When Jurkat cells are infected with a plasmid containing an infectious full-length HIV-1 and continuously exposed to 10 μM AME escape mutants indicate mutations in an endocytoses motif in the cytoplasmic part of gp41, the viral fusion protein (Waheed et al., 2006). In another study, it has been shown that AME lowers virus production (Waheed et al., 2008). AME seems to be noneffective against the Gag-membrane protein assembly and Gag-association with detergent-resistant membranes. It rather lowers the amount of virion release by approximately fivefold. Vpu-deficient HIV mutants are insensitive to AME treatment also in the presence of an overexpression of CD317/BST-2/tetherin. Reinjection of the cells with Vpu plasmid makes the cell sensitive to AME again. This indicates that AME most likely disrupts the Vpu-CD317/DST-2/tetherin interaction. It is speculated that AME blocks ion channel activity of Vpu. Further, it may be speculated that Vpu may need raft association to be fully functional.

This study (Waheed et al., 2006, 2008) shows that there could also be a conceptual different pathway to block a membrane protein. It could be anticipated that AME locates itself at those sites of lipid rafts which "show" the cholesterol, and with this, the interaction of Vpu or other viral proteins with these sites is not possible anymore. If AME does not interact with Vpu, it cannot act as a "replacement" of cholesterol and Vpu function is abrogated.

4.9. Cholesterol depleting drugs

Lipid membrane composition is an integral part for the mechanism of function of some of the VCPs such as M2 and Vpu. Especially, the latter is found in lipid rafts. Since rafts are lipid patches with a high content of cholesterol, cholesterol depleting drugs are suggested to combat the virus (Ruiz et al., 2010b). Experiments have shown that cells which express Vpu but are treated with a combination of lovastatin and M-β-CD show reduced levels of Vpu in detergent-resistant membrane microdomains.

4.10. Anti-raft and plant-derived drugs

It has been shown that lipid composition and with it the existence of rafts is essential for viral entry and budding (Brügger et al., 2006). Anti-raft drugs have been proposed to target rafts and with it especially to combat the replication of HIV-1 (Verma, 2009). Plant-derived drugs have been found exhibiting potential preventive effects of HIV-1 progression. Compounds such as ω-3-fatty acids and plant-derived triterpenes are investigated. Since

involvement of rafts in the mechanism of function of the viral channels is gradually emerging, these drug candidates could potentially be affecting the VCPs.

Other plant-derived drugs such as polyphenols are proposed to target extramembrane parts of channel proteins while lipophilic terpenoids act within the membrane either directly or indirectly (Wink, 2008). Saponins target cholesterol and could also act in a dual mode as mentioned: directly by protein–drug interaction or by an indirect mode of action, such as distorting raft composition. It is up to further studies to modify these candidates to address them more specifically to viral channels.

A promising plant-derived drug candidate is emodin (6-methyl-1,3,8-trihydroxyanthraquinone, Fig. 6.6), targeting 3a not only of SARS-CoV but also HCoV-OC43 (Schwarz et al., 2011). The binding constant has been calculated to be 20 μM using voltage clamp conditions on *Xenopus* oocytes expressing 3a.

4.11. Remarks

To date, M2 is the only target channel protein used in antiviral therapy. Protein p7 and eventually Vpu are in closer reach. For other proteins, investigations are still very much on a laboratory level reporting interactions of known drugs with the channel proteins.

5. Overall Summary and Outlook

The current findings on the viral channel-forming proteins are reviewed in respect of the mechanism of function and their role of affecting electrochemical or substrate gradients. While for M2, a detailed picture of the mechanics of proton translocation is emerging due to structural work, the reason for weak cation selectivity of most of the channels is still in the dark. Based on sequence alignment studies, a relation to host channels and toxins is drawn for some of the channel proteins. With Vpu relating to toxin ClyA, and ditopic channels like p7 and 2B relating to McsL and tritopic 3a likely to ligand-gated channels, the picture emerges that this type of protein covers the range from pores to channels. M2 as a proton channel may "borrow" mechanisms from other proton conducting and translocating membrane proteins. The evidence is growing that some of these proteins are raft associated. Also, the evidence emerges that channel functionality is not the only role these proteins inherit. Many of them interact with host factors to steer the cell toward the benefit of the virus (stage of steering). Questions arise whether this "steering of the host" is done as monomeric or oligomeric units. In addition to it, there is some kind of equilibrium

between the "stage of steering" and the proper channel state as an oligomeric unit. Or is the interaction with the host to be seen as a kind of "host based ligand" closing the channel while without the host protein the channel is open; or do other ligands trigger activity? More surprising, with influenza A and SARS-CoV two viruses emerge which harbor more than one channel protein. On the other end of this scale, for Dengue virus there is no report of any channel protein up to now despite its membership to the same family, *Flaviviridae*, as HCV.

Drug development is yet still to be fully explored. With M2 as the only target so far, two more channel proteins are on the horizon to be potential candidates. Since structural information is sparse for most of the channels, development of pore occluding drugs is difficult. Drug–protein interaction seems to obey, in the same sophisticated way as for any other host or protein of pathogens, allosteric binding modes. On the other hand, drug development is challenged, due to the fact that protein–protein interactions between viral and host proteins are also happening within the lipid membrane. Thus, novel concepts for finding drugs are essential. This may put peptide drugs, peptidomimetics, and plant-derived drugs in an elevated position for lead discovery.

ACKNOWLEDGMENTS

W. B. F. acknowledges financial support from the National Science Council (NSC) of Taiwan (NSC98-2112-M-010-002-MY3). C. S. thanks for a fellowship of the Alfried Krupp von Bohlen und Halbach Foundation and the German National Academic Foundation. Thanks to Hao-Jen Hsu, Li-Hua Li, Meng-Han Lin, Tze-Hsiang Chien, Yi-Ching Yang, Chao-Lung Wang, and Roman Schilling for valuable discussions.

REFERENCES

Abenavoli, A., DiFrancesco, M.L., Schroeder, I., Epimashko, S., Gazzarrini, S., Hansen, U. P., et al., 2009. Fast and slow gating are inherent properties of the pore module of the K+ channel Kcv. J. Gen. Physiol. 134, 219–229.

Acharya, R., Carnevale, V., Fiorin, G., Levine, B.G., Polishchuk, A.L., Balannik, V., et al., 2010. Structure and mechanism of proton transport through the transmembrane tetrameric M2 protein bundle of the influenza A virus. Proc. Natl. Acad. Sci. USA 107, 15075–15080.

Agerberth, B., Gunne, H., Odeberg, J., Kogner, P., Boman, H.G., Gudmundsson, G.H., 1995. FALL-39, a putative human peptide antibiotic, is cystein-free and expressed in bone marrow and testis. Proc. Natl. Acad. Sci. USA 92, 195–199.

Agyei, D., Danquah, M.K., 2011. Industrial-scale manufacturing of pharmaceutical-grade bioactive peptides. Biotechnol. Adv. 29, 272–277.

Aldabe, R., Barco, A., Carrasco, L., 1996. Membrane permeabilization by poliovirus proteins 2B and 2BC. J. Biol. Chem. 271, 23134–23137.

Allen, H., McCauley, J., Waterfield, M., Gethering, M., 1980. Influenza virus RNA segment 7 has the coding capacity for two polypeptides. Virology 107, 548–551.

Aloia, R.C., Tian, H., Jensen, F.C., 1993. Lipid composition and fluidity of the human immunodeficiency virus envelope and host cell plasma membrane. Proc. Natl. Acad. Sci. USA 90, 5181–5185.

Anishkin, A., Sukharev, S., 2009. State-stabilizing interactions in bacterial mechanosensitive channel gating and adaptation. J. Biol. Chem. 284, 19153–19157.

Arbely, E., Khattari, Z., Brotons, G., Akkawi, M., Salditt, T., Arkin, I.T., 2004. A highly unusual palindromic transmembrane helical hairpin formed by SARS coronavirus E protein. J. Mol. Biol. 341, 769–779.

Balannik, V., Lamb, R.A., Pinto, L.H., 2008. The oligomeric state of the active BM2 ion channel protein of influenza B virus. J. Biol. Chem. 283, 4895–4904.

Bass, R.B., Strop, P., Barclay, M., Rees, D.C., 2002. Crystal structure of Escherichia coli MscS, a voltage-modulated and mechanosensitive channel. Science 298, 1582–1587.

Becker, C.F.W., Oblatt-Montal, M., Kochendoerfer, G.G., Montal, M., 2004. Chemical synthesis and single channel properties of tetrameric and pentameric TASPs (template-assembled synthetic proteins) derived from the transmembrane domain of HIV virus protein u (Vpu). J. Biol. Chem. 279, 17483–17489.

Beckstein, O., Sansom, M.S.P., 2006. A hydrophobic gate in an ion channel: the closed state of the nicotinic acetylcholine receptor. Phys. Biol. 3, 147–159.

Belshe, R.B., Burk, B., Newman, F., Cerruti, R.L., Sim, I.S., 1989. Resistance of influenza A virus to amantadine and rimantadine: results of one Decade of surveillance. J. Infect. Dis. 159, 430–435.

Beniac, D.R., Andonov, A., Grudeski, E., Booth, T.F., 2006. Architecture of the SARS coronavirus prefusion spike. Nat. Struct. Mol. Biol. 13, 751–752.

Bolduan, S., Votteler, J., Lodermeyer, V., Greiner, T., Koppensteiner, H., Schindler, M., et al., 2011. Ion channel activity of HIV-1 Vpu is dispensable for counteraction of CD317. Virology 416, 75–85.

Bour, S., Strebel, K., 2003. The HIV-1 Vpu protein: a multifunctional enhancer of viral particle release. Microbes Infect. 5, 1029–1039.

Bour, S., Schubert, U., Strebel, K., 1995. The human immunodeficiency virus type 1 Vpu protein specifically binds to the cytoplasmic domain of CD4: implications for the mechanism of degradation. J. Virol. 69, 1510–1520.

Briedis, D.J., Lamb, R.A., Choppin, P.W., 1982. Sequence of RNA segment 7 of the influenza B virus genome: partial amino acid identity between the membrane protein (M1 of influenza A and B viruses and conservation of a second open reading frame. Virology 116, 581–588.

Brügger, B., Glass, B., Haberkant, P., Leibrecht, I., Wieland, F.T., Kräusslich, H.-G., 2006. The HIV lipidome: a raft with an unusual composition. Proc. Natl. Acad. Sci. USA 103, 2641–2646.

Bruns, K., Studtrucker, N., Sharma, A., Fossen, T., Mitzner, D., Eissmann, A., et al., 2007. Structural characterization and oligomerization of PB1-F2, a pro-apoptotic influenza A virus protein. J. Biol. Chem. 282, 353–363.

Cady, S.D., Mishana, T.V., Hong, M., 2009. Structure of amantadine-bound M2 transmembrane peptide of influenza A in lipid bilayers from magic-angle-spinning solid-state NMR: the role of Ser31 in amantadine binding. J. Mol. Biol. 385, 1127–1141.

Cady, S.D., Schmidt-Rohr, K., Wang, J., Soto, C.S., DeGrado, W.F., Hong, M., 2010. Structure of the amantadine binding site of influenza M2 proton channels in lipid bilayers. Nature 463, 689–692.

Callahan, M.A., Handley, M.A., Lee, Y.-H., Talbot, K.J., Harper, J.W., Panganiban, A.T., 1998. Functional interaction of human immunodeficiency virus type 1 Vpu and Gag with a novel membrane of the tetratricopeptide repeat protein family. J. Virol. 72, 5189–5197.

Campbell, S.M., Crowe, S.M., Mak, J., 2001. Lipid rafts and HIV-1: from viral entry to assembly of progeny virions. J. Clin. Virol. 22, 217–227.

Carnevale, V., Fiorin, G., Levine, B.G., DeGrado, W.F., Klein, M.L., 2010. Multiple proton confinement in the M2 channel from the influenza A virus. J. Phys. Chem. C Nanomater. Interfaces 114, 20856–20863.

Carrasco, L., 1995. Modification of membrane permeability by animal viruses. Adv. Virus Res. 45, 61–112.

Carrère-Kremer, S., Montpellier-Pala, C., Cocquerel, L., Wychowski, C., Penin, F., Dubuisson, J., 2002. Subcellular localization and topology of the p7 polypeptide of Hepatitis C virus. J. Virol. 76, 3720–3730.

Chang, G., Spencer, R.H., Lee, A.T., Barclay, M.T., Rees, D.C., 1998. Structure of the MscL homolog from Mycobacterium tuberculosis: a gated mechanosensitive ion channel. Science 282, 2220–2226.

Chanturiya, A.N., Basanez, G., Schubert, U., Henklein, P., Yewdell, J.W., Zimmerberg, J., 2004. Pb1-F2, an influenza A virus-encoded proapoptotic mitochondrial protein, creates variably sized pores in planar lipid membranes. J. Virol. 78, 6304–6312.

Chen, J., Cassar, S.C., Zhang, D.H., Gopalakrishnan, M., 2005. A novel potassium channel encoded by *Ectocarpus siliculosus* virus. Biochem. Biophys. Res. Commun. 326, 887–893.

Chen, C.-Y., Ping, Y.-H., Lee, H.-C., Chen, K.-H., Lee, Y.-M., Chan, Y.-J., et al., 2007a. Open reading frame 8a of the Human severe acute respiratory syndrome coronavirus not only promotes viral replication but also induces apoptosis. J. Infect. Dis. 196, 405–415.

Chen, H., Wu, Y., Voth, G.A., 2007b. Proton transport behaviour through the Influenza A M2 channel: insights from molecular simulations. Biophys. J. 93, 3470–3479.

Chen, Y., Wang, M., Zhang, Q., Liu, J., 2010. Construction of an implicit membrane environment for the lattice Monte Carlo simulation of transmembrane protein. Biophys. Chem. 147, 35–41.

Chen, C.C., Krüger, J., Sramala, I., Hsu, H.J., Henklein, P., Chen, Y.M.A., et al., 2011. ORF 8a of severe acute respiratory syndrome coronavirus forms an ion channel: experiments and molecular dynamics simulations. Biochim. Biophys. Acta 1808, 572–579.

Chew, C.F., Vijayan, R., Chang, J., Zitzmann, N., Biggin, P.C., 2009. Determination of pore-lining residues in the hepatitis C virus p7 protein. Biophys. J. 96, L10–L12.

Chizhmakov, I.V., Geraghty, F.M., Ogden, D.C., Hayhurst, A., Antoniou, M., Hay, A.J., 1996. Selctive proton permeability and pH regulation of the influenza virus M2 channel expressed in mouse erythroleukaemia cells. J. Physiol. 494, 329–336.

Clarke, D., Griffin, S., Beales, L., Gelais, C.S., Burgess, S., Harris, M., et al., 2006. Evidence for the formation of a heptameric ion channel complex by the hepatitis C virus p7 protein in vitro. J. Biol. Chem. 281, 37057–37068.

Coadou, G., Evrard-Todeschi, N., Gharbi-Benarous, J., Benarous, R., Girault, J.-P., 2001. Conformational analysis by NMR and molecular modelling of the 41–62 hydrophilic region of HIV-1 encoded virus protein U (Vpu). Effect of the phosphorylation on sites 52 and 56. C. R. Acad. Sci. Paris, Chemie / Chemistry 4, 751–758.

Coadou, G., Evrard-Todeschi, N., Gharbi-Benarous, J., Benarous, R., Girault, J.-P., 2002. HIV-1 encoded virus protein U (Vpu) solution structure of the 41–62 hydrophilic region containing the phosphorylated sites Ser^{52} and Ser^{56}. Int. J. Biol. Macromol. 30, 23–40.

Coady, M.J., Daniel, N.G., Tiganos, E., Allain, B., Friborg, J., Lapointe, J.-Y., et al., 1998. Effects of Vpu expression on Xenopus oocyte membrane conductance. Virology 244, 39–49.

Cohen, E.A., Terwilliger, E.F., Sodroski, J.G., Haseltine, W.A., 1988. Identification of a protein encoded by the *vpu* gene of HIV-1. Nature 334, 532–534.

Cook, G.A., Opella, S.J., 2010. NMR studies of the p7 protein from Hepatitis C virus. Eur. Biophys. J. 39, 1097–1104.

Cook, G.A., Opella, S.J., 2011. Secondary structure, dynamics, and architecture of the p7 membrane protein from hepatitis C virus by NMR spectroscopy. Biochim. Biophys. Acta 1808, 1448–1453.

Cordes, F., Kukol, A., Forrest, L.R., Arkin, I.T., Sansom, M.S.P., Fischer, W.B., 2001. The structure of the HIV-1 Vpu ion channel: modelling and simulation studies. Biochim. Biophys. Acta 1512, 291–298.

Cordes, F.S., Tustian, A.D., Sansom, M.S., Watts, A., Fischer, W.B., 2002. Bundles consisting of extended transmembrane segments of Vpu from HIV-1: computer simulations and conductance measurements. Biochemistry 41, 7359–7365.

Cuconati, A., Xiang, W., Lahser, F., Pfister, T., Wimmer, E., 1998. A protein linkage map of the P2 nonstructural proteins of poliovirus. J. Virol. 72, 1297–1307.

Cuthbertson, J.M., Doyle, D.A., Sansom, M.S.P., 2005. Transmembrane helix prediction: a comparative evaluation and analysis. Protein Eng. Des. Sel. 18, 295–308.

Cymes, G.D., Grosman, C., 2008. Pore-opening mechanism of the nicotinic acetylcholine receptor evinced by proton transfer. Nat. Struct. Mol. Biol. 15, 389–396.

Czabotar, P.E., Martin, S.R., Hay, A.J., 2004. Studies of structural changes in the M2 proton channel of influenza A virus by tryptophan fluorescence. Virus Res. 99, 57–61.

Davies, W.L., Grunert, R.R., Haff, R.F., McGahen, J.W., Neumayer, E.M., Paulshock, M., et al., 1964. Antiviral activity of 1-adamantanamine (amantadine). Science 144, 862–863.

de Jong, A.S., Schrama, I.W., Willems, P.H., Galama, J.M., Melchers, W.J., van Kuppeveld, F.J., 2002. Multimerization reactions of coxsackievirus proteins 2B, 2C and 2BC: a mammalian two-hybrid analysis. J. Gen. Virol. 83, 783–793.

de Jong, A.S., Visch, H.-J., de Mattia, F., van Dommelen, M.M., Swart, H.G., Luyten, T., et al., 2006. The coxsackievirus 2B protein increases efflux of ions from the endoplasmic reticulum and Golgi, thereby inhibiting protein trafficking through the Golgi. J. Biol. Chem. 281, 14144–14150.

Debnath, A.K., 2006. Progress in identifying peptides and small-molecule inhibitors targeted to gp41 of HIV-1. Expert Opin. Investig. Drugs 15, 465–478.

DeCoursey, T.E., 2008. Voltage-gated proton channels. Cell. Mol. Life Sci. 65, 2554–2573.

Deltenre, P., Henrion, J., Canva, V., Dharancy, S., Texier, F., Louvet, A., et al., 2004. Evaluation of amantadine in chronic hepatitis C: a meta-analysis. J. Hepatol. 41, 462–473.

Deyde, V.M., Xu, X., Bright, R.A., Shaw, M., Smith, C.B., Zhang, Y., et al., 2007. Surveillance of resistance to adamantanes among influenza A (H3N2) and A (H1N1) virus isolated worldwide. J. Infect. Dis. 196, 249–257.

Doedens, J.R., Kirkegaard, K., 1995. Inhibition of cellular protein secretion by poliovirus proteins 2B and 3A. EMBO J. 14, 894–907.

Doyle, D.A., Cabral, J.M., Pfuetzner, R.A., Kuo, A., Gulbis, J.M., Cohen, S.L., et al., 1998. The structure of the potassium channel: molecular basis of K^+ conduction and selectivity. Science 280, 69–77.

Dubé, M., Roy, B.B., Guiot-Guillain, P., Binette, J., Mercier, J., Chiasson, A., et al., 2010. Antagonism of tetherin restriction of HIV-1 release by Vpu invovles binding and sequestration of the restriction factor in a perinuclear compartment. PLoS Pathog. 6, e1000856.

Duff, K.C., Ashley, R.H., 1992. The transmembrane domain of influenza A M2 protein forms amantadine-sensitive proton channels in planar lipid bilayers. Virology 190, 485–489.

Duff, K.C., Kelly, S.M., Price, N.C., Bradshaw, J.P., 1992. The secondary structure of influenza A M2 transmembrane domain. A circular dichroism study. FEBS Lett. 311, 256–258.

Duff, K.C., Gilchrist, P.J., Saxena, A.M., Bradshaw, J.P., 1994. Neutron diffraction reveals the site of amantadine blockade in the influenza A M2 ion channel. Virology 202, 287–293.

Eckert, D.M., Kim, P.S., 2001. Mechanisms of viral membrane fusion and its inhibition. Annu. Rev. Biochem. 70, 777–810.

Edman, K., Nollert, P., Royant, A., Belrhali, H., Pebay-Peyroula, E., Hajdu, J., et al., 1999. High-resolution X-ray structure of an early intermediate in the bacteriorhodopsin photocycle. Nature 401, 822–826.

Elbers, K., Tautz, N., Becher, P., Stoll, D., Rumenapf, T., Thiel, H.J., 1996. Processing in the pestivirus E2-NS2 region: identification of proteins p7 and E2p7. J. Virol. 70, 4131–4135.

Ewart, G.D., Sutherland, T., Gage, P.W., Cox, G.B., 1996. The Vpu protein of human immunodeficiency virus type 1 forms cation-selective ion channels. J. Virol. 70, 7108–7115.

Ewart, G.D., Mills, K., Cox, G.B., Gage, P.W., 2002. Amiloride derivatives block ion channel activity and enhancement of virus-like particle budding caused by HIV-1 protein Vpu. Eur. Biophys. J. 31, 26–35.

Federau, T., Schubert, U., Floßdorf, J., Henklein, P., Schomburg, D., Wray, V., 1996. Solution structure of the cytoplasmic domain of the human immunodeficiency virus type 1 encoded virus protein U (Vpu). Int. J. Pept. Protein Res. 47, 297–310.

Fischer, W.B., 2003. Vpu from HIV-1 on an atomic scale: experiments and computer simulations. FEBS Lett. 552, 39–46.

Fischer, W.B. (2005). Viral membrane proteins: structure, function and drug design. In: Atassi, M.Z. (Ed.), Protein Reviews. Kluwer Academic/Plenum Publisher, New York, pp. 291.

Fischer, W.B., Hsu, H.J., 2011. Viral channel forming proteins—modelling the target. Biochim. Biophys. Acta 1808, 561–571.

Fischer, W.B., Krüger, J., 2009. Viral channel forming proteins. Int. Rev. Cell Mol. Biol. 275, 35–63.

Fischer, W.B., Sansom, M.S.P., 2002. Viral ion channels: structure and function. Biochim. Biophys. Acta 1561, 27–45.

Fischer, W.B., Sonar, S., Marti, T., Khorana, H.G., Rothschild, K.J., 1994. Detection of a water molecule in the active-site of Bacteriorhodopsin: hydrogen bonding changes during the primary photoreaction. Biochemistry 33, 12757–12762.

Forssmann, W.-G., The, Y.-H., Stoll, M., Adermann, K., Albrecht, U., Barlos, K., et al., 2010. Short-term monotherapy in HIV-infected patients with a virus entry inhibitor against the gp41 fusion peptide. Sci. Transl. Med. 63, 63re3.

Foster, T.L., Verow, M., Wozniak, A.L., Bentham, M.J., Thompson, J., Atkins, E., et al., 2011. Resistance mutations define specific antiviral effects for inhibitors of the hepatitis C virus p7 ion channel. Hepatology 54, 79–90.

Franco, R., Bortner, C.D., 2006. Potential roles of electrogenic ion transport and plasma membrane depolarization in apoptosis. J. Membr. Biol. 209, 43–58.

Gaedigk-Nitschko, K., Ding, M.X., Levy, M.A., Schlesinger, M.J., 1990. Site-directed mutations in the sinbis virus 6K protein reveal sites for fatty acylation and the underactlated protein affects virus release and virion structure. Virology 175, 282–291.

Gandhi, C.S., Shuck, K., Lear, J.D., Dieckmann, G.R., DeGrado, W.F., Lamb, R.A., et al., 1999. Cu(II) inhibition of the proton translocation machinery of the influenza A virus M2 protein. J. Biol. Chem. 274, 5474–5482.

Garoff, H., Kondor-Koch, C., Riedel, H., 1982. Structure and assembly of alphaviruses. Curr. Top. Microbiol. Immunol. 99, 1–50.

Gazzarrini, S., Severino, M., Lombardi, M., Morandi, M., DiFrancesco, D., Van Etten, J.L., et al., 2003. The viral potassium channel Kcv: structural and functional features. FEBS Lett. 552, 12–16.

Gazzarrini, S., Kang, M., van Etten, J.L., Tayefeh, S., Kast, S.M., DiFrancesco, D., et al., 2004. Long distance interactions within the potassium channel pore are revealed by molecular diversity of viral proteins. J. Biol. Chem. 279, 28443–28449.

Godballe, T., Nilsson, L.L., Petersen, P.D., Jenssen, H., 2011. Antimicrobial b-peptides and a-peptoids. Chem. Biol. Drug Des. 77, 107–116.

Gonzales, M.E., Carrasco, L., 1998. The human immunodeficiency virus type 1 Vpu protein enhances membrane permeability. Biochemistry 37, 13710–13719.

Gonzales, M.E., Carrasco, L., 2003. Viroporins. FEBS Lett. 552, 28–34.

Grice, A.L., Kerr, I.D., Sansom, M.S.P., 1997. Ion channels formed by HIV-1 Vpu: a modelling and simulation study. FEBS Lett. 405, 299–304.

Griffin, S.D.C., 2009. Plugging the holes in hepatitis C virus antiviral therapy. Proc. Natl. Acad. Sci. USA 106, 12567–12568.

Griffin, S.D.C., Beales, L.P., Clarke, D.S., Worsfold, O., Evans, S.D., Jäger, J., et al., 2003. The p7 protein of hepatitis C virus forms an ion channel that is blocked by the antiviral drug, amantadine. FEBS Lett. 535, 34–38.

Guan, Y., Zheng, B.-J., He, Y.Q., Liu, X.L., Zhuang, Z.X., Cheung, C.L., et al., 2003. Isolation and characterization of viruses related to the SARS Coronavirus from animals in southern China. Science 302, 276–278.

Harada, T., Tautz, N., Thiel, H.J., 2000. E2-p7 region of the bovine viral diarrhea virus polyprotein: processing and functional studies. J. Virol. 74, 9498–9506.

Hay, A.J., Wolstenholme, A.J., Skehel, J.J., Smith, M.H., 1985. The molecular basis of the specific anti-influenza action of amantadine. EMBO J. 4, 3021–3024.

Henderson, R., Baldwin, J.M., Ceska, T.A., Zemlin, F., Beckmann, E., Downing, K.H., 1990. Model for the structure of bacteriorhodopsin based on high-resolution electron cryo-microscopy. J. Mol. Biol. 213, 899–929.

Henkel, M., Mitzner, D., Henklein, P., Meyer-Almes, F.-J., Moroni, A., DiFrancesco, M.L., et al., 2010. The proapoptotic Influenza A virus protein PB1-F2 forms a nonselective ion channel. PLoS One 5, e11112.

Herzfeld, J., Lansing, J.C., 2002. Magnetic resonance studies of the bacteriorhodopsin pump cycle. Annu. Rev. Biophys. Biomol. Struct. 31, 73–95.

Hiebert, S.W., Williams, M.A., Lamb, R.A., 1986. Nucleotide sequence of RNA segment 7 of influenza B/Singapore/22/79: maintenance of a second large open reading frame. Virology 155, 747–751.

Hilf, R.J.C., Dutzler, R., 2008. X-ray structure of a prokaryotic pentameric ligand-gated ion channel. Nature 452, 375–379.

Hilf, R.J.C., Dutzler, R., 2009. Structure of a potentially open state of a proton-activated pentameric ligand-gated ion channel. Nature 457, 115–119.

Hinz, A., Miguet, N., Natrajan, G., Usami, Y., Yamanaka, H., Renesto, P., et al., 2010. Structural basis of HIV-1 tethering to membranes by the BST-2/tetherin ectodomain. Cell Host Microbe 7, 314–323.

Holsinger, L.J., Lamb, R.A., 1991. Influenza virus M2 integral membrane protein is a homotetramer stabilized by formation of disulphide bonds. Virology 183, 32–43.

Horvath, C.M., Williams, M.A., Lamb, R.A., 1990. Eukaryotic coupled translation of tandem cistrons: identification of the influenza B virus BM_2 polypeptide. EMBO J. 9, 2639–2647.

Hsu, H.-J., Fischer, W.B., 2011. In silico investigations of possible routes of assembly of ORF 3a from SARS-CoV. J. Mol. Model. (May 4 [Epub ahead of print] online first).

Hsu, K., Seharaseyon, J., Dong, P., Bour, S., Marbán, E., 2004. Mutual functional destruction of HIV-1 Vpu and host TASK-1 channel. Mol. Cell 14, 259–267.

Hsu, K., Han, J., Shinlapawittayatorn, K., Deschenes, I., Marbán, E., 2010. Membrane potential depolarization as a triggering mechanism for Vpu-mediated HIV-1 release. Biophys. J. 99, 1718–1725.

Hu, J., Fu, R., Nishimura, K., Zhang, L., Zhou, H.-X., Busath, D.D., et al., 2006. Histidines, heart of the hydrogen ion channel from influenza A virus: toward an understanding of conductance and proton selectivity. Proc. Natl. Acad. Sci. USA 103, 6865–6870.

Hu, J., Asbury, T., Achuthan, S., Bertram, R., Quine, J.R., Fu, R., et al., 2007. Backbone structure of the amantadine-blocked trans-membrane domain M2 protein channel from influenza A virus. Biophys. J. 92, 4335–4343.

Hu, F., Luo, W., Cady, S.D., Hong, M., 2011. Conformational plasticity of the influenza A M2 transmembrane helix in lipid bilayers under varying pH, drug binding, and membrane thickness. Biochim. Biophys. Acta 1808, 415–423.

Huang, H.W., 2000. Action of antimicrobial peptides: two-state model. Biochemistry 39, 8347–8352.

Huang, C., Narayanan, K., Ito, N., Peters, C.J., Makino, S., 2006. Sever acute respiratory syndrome coronavirus 3a protein is released in membranous structures from 3a protein-expressing cells and infected cells. J. Virol. 80, 210–217.

Hussain, A., Das, S.R., Tanwar, C., Jameel, S., 2007. Oligomerization of the human immunodeficiency virus type I (HIV-1) Vpu protein—a genetic, biochemical and biophysical analysis. Virol. J. 4, 1–11.

Hussain, A., Wesley, C., Khalid, M., Chaudhry, A., Jameel, S., 2008. Human immunodeficiency virus type 1 Vpu protein interacts with CD74 and modulates major histocompatibility complex class II presentation. J. Virol. 82, 893–902.

Iacovache, I., van der Goot, F.G., Pernot, L., 2008. Pore formation: an ancient yet complex form of attack. Biochim. Biophys. Acta 1778, 1611–1623.

Ito, N., Mossel, E.C., Narayanan, K., Popov, V.L., Huang, C., Inoue, T., et al., 2005. Severe acute respiratory syndrome coronavirus 3a protein is a viral structural protein. J. Virol. 79, 3182–3186.

Jiang, Y., Lee, A., Chen, J., Cadene, M., Chait, B.T., MacKinnon, R., 2002a. Crystal structure and mechanism of a calcium-gated potassium channel. Nature 417, 515–522.

Jiang, Y., Lee, A., Chen, J., Cadene, M., Chait, B.T., MacKinnon, R., 2002b. The open pore conformation of potassium channels. Nature 417, 523–526.

Jones, C.T., Murray, C.L., Eastman, D.K., Tassello, J., Rice, C.M., 2007. Hepatitis C virus p7 and NS2 proteins are essential for production of infectious virus. J. Virol. 81, 8374–8383.

Khoury, G., Ewart, G., Luscombe, C., Miller, M., Wilkinson, J., 2010. Antiviral efficacy of the novel compound BIT225 against HIV-1 release from human macrophages. Antimicrob. Agents Chemother. 54, 835–845.

Khurana, E., Dal Peraro, M., De Vane, R., Vemparala, S., DeGrado, W.F., Klein, M.L., 2009. Molecular dynamics calculations suggest a conductance mechanism for the M2 proton channel from influenza A virus. Proc. Natl. Acad. Sci. USA 106, 1069–1074.

Kim, S., Jeon, T.-J., Oberai, A., Yang, D., Schmidt, J.J., Bowie, J.U., 2005. Transmembrane glycine zippers: physiological and pathological roles in membrane proteins. Proc. Natl. Acad. Sci. USA 102, 14278–14283.

Kim, C.G., Lemaitre, V., Watts, A., Fischer, W.B., 2006. Drug-protein interaction with Vpu from HIV-1: proposing binding sites for amiloride and one of its derivatives. Anal. Bioanal. Chem. 386, 2213–2217.

Kloda, A., Petrov, E., Meyer, G.R., Nguyen, T., Hurst, A.C., Hool, L., et al., 2008. Mechanosensitive channel of large conductance. Int. J. Biochem. Cell Biol. 40, 164–169.

Kötting, C., Gerwert, K., 2005. Proteins in action monitored by time-resolved FTIR spectroscopy. Chemphyschem 6, 881–888.

Kovacs, F.A., Cross, T.A., 1997. Transmembrane four-helix bundle of influenza A M2 protein channel: structural implications from helix tilt and orientation. Biophys. J. 73, 2511–2517.

Krüger, J., Fischer, W.B., 2008. Exploring the conformational space of Vpu from HIV-1: a versatile and adaptable protein. J. Comput. Chem. 29, 2416–2424.
Krüger, J., Fischer, W.B., 2009. Assembly of viral membrane proteins. J. Chem. Theory Comput. 5, 2503–2513.
Kukol, A., Arkin, I.T., 1999. Vpu transmembrane peptide structure obtained by site-specific fourier transform infrared dichroism and global molecular dynamics searching. Biophys. J. 77, 1594–1601.
Kukol, A., Adams, P.D., Rice, L.M., Brunger, A.T., Arkin, I.T., 1999. Experimentally based orientational refinement of membrane protein models: a structure for the influenza A M2 H^+ channel. J. Mol. Biol. 286, 951–962.
Kuo, A., Gulbis, J.M., Antcliff, J.F., Rahman, T., Lowe, E.D., Zimmer, J., et al., 2003. Crystal structure of the potassium channel KirBac1.1 in the closed state. Science 300, 1922–1926.
Lamb, R.A., Choppin, P.W., 1981. Identification of a second protein (M_2) encoded by RNA segment 7 of Influenza virus. Virology 112, 729–737.
Lamb, R.A., Lai, C.-J., 1981. Conservation of the influenza virus membrane proteins (M_1) amino acid sequence and an open readig frame of RNA segment 7 encoding a second protein (M_2) in H1N1 and H3N2 strains. Virology 112, 746–751.
Lamb, R.A., Pinto, L.H., 1997. Do Vpu and Vpr of human immunodeficiency virus type 1 and NB of influenza B virus have ion channel activities in the viral life cycles? Virology 229, 1–11.
Lamb, R.A., Zebedee, S.L., Richardson, C.D., 1985. Influenza virus M2 protein is an integral membrane protein expressed on the infected-cell surface. Cell 40, 627–633.
Langosch, D., Arkin, I.T., 2009. Interaction and conformational dynamics of membrane-spanning protein helices. Protein Sci. 18, 1343–1358.
Le Novère, N., Changeux, J.P., 1995. Molecular evolution of the nicotinic acetylcholine receptor: an example of multigene family in excitable cells. J. Mol. Evol. 40, 155–172.
Lemaitre, V., Willbold, D., Watts, A., Fischer, W.B., 2006. Full length Vpu from HIV-1: combining molecular dynamics simulations with NMR spectroscopy. J. Biomol. Struct. Dyn. 23, 485–496.
Li, C., Qin, H., Gao, F.P., Cross, T.A., 2007. solid-state NMR characterization of conformational plasticity within the transmembrane domain of the influenza A M2 proton channel. Biochim. Biophys. Acta 1768, 3162–3170.
Liao, Y., Yuan, Q., Torres, J., Tam, J.P., Liu, D.X., 2006. Biochemical and functional characterization of the membrane association and membrane permeabilizing activity of the severe acute respiratory syndrome coronavirus envelope protein. Virology 349, 264–275.
Liljestrom, P., Garoff, H., 1991. Internally located cleavable signal sequences direct the formation of semliki forest virus membrane proteins from a polyprotein precursor. J. Virol. 65, 147–154.
Lin, T., Schroeder, C., 2001. Definitive assignment of proton selectivity and attoampere unitary current to the M2 ion channel protein of influenza A virus. J. Virol. 75, 3647–3656.
Lin, C., Lindenbach, B.D., Pragai, B.M., McCourt, D.W., Rice, C.M., 1994. Processing in the hepatitis C virus E2-NS2 region: identification of p7 and two distinct E2-specific products with different C termini. J. Virol. 68, 5063–5073.
Liu, Z., Gandhi, C.S., Rees, D.C., 2009. Structure of a tetrameric MscL in an expanded intermediate state. Nature 461, 120–124.
Lohmann, V., Korner, F., Koch, J., Herian, U., Theilmann, L., Bartenschlager, R., 1999. Replication of subgenomic hepatitis C virus RNAs in a hepatoma cell line. Science 285, 110–113.
Lopez, C.F., Montal, M., Blasie, J.K., Klein, M.L., Moore, P.B., 2002. Molecular dynamics investigation of membrane-bound bundles of the channel-forming transmembrane

domain of viral protein U from the Human Immunodeficiency Virus HIV-1. Biophys. J. 83, 1259–1267.

Lu, W., Zheng, B.-J., Xu, K., Schwarz, W., Du, L., Wong, C.K.L., et al., 2006. Severe acute respiratory syndrome-associated coronavirus 3a protein forms an ion channel and modulates virus release. Proc. Natl. Acad. Sci. USA 103, 12540–12545.

Luik, P., Chew, C., Aittoniemi, J., Chang, J., Wentworth Jr., P., Dwek, R., et al., 2009. The 3-dimensional structure of the hepatitis C virus p7 ion channel by electron microscopy. Proc. Natl. Acad. Sci. USA 106, 12712–12716.

Lusa, S., Garoff, H., Liljeström, P., 1991. Fate of the 6K membrane protein of smliki forest virus during virus assembly. Virology 185, 843–846.

Luscombe, C.A., Huang, Z., Murray, M.G., Miller, M., Wilkinson, J., Ewart, G.D., 2010. A novel Hepatitis C virus p7 ion channel inhibitor, BIT225, inhibits bovine viral diarrhea virus *in vitro* and shows synergism with recombinant interferon-a-2b and nucleaoside analogues. Antiviral Res. 86, 144–153.

Ma, C., Marassi, F.M., Jones, D.H., Straus, S.K., Bour, S., Strebel, K., et al., 2002. Expression, purification, and activities of full-length and truncated versions of the integral membrane protein Vpu from HIV-1. Protein Sci. 11, 546–557.

Ma, C., Soto, C.S., Ohigashi, Y., Taylor, A., Bournas, V., Glawe, B., et al., 2008. Identification of the pore-lining residues of the BM2 ion channel protien of influenza B virus. J. Biol. Chem. 283, 15921–15931.

Ma, Y., Anantpadma, M., Timpe, J.M., Shanmugam, S., Singh, S.M., Lemon, S.M., et al., 2011. Hepatitis C virus NS2 protein serves as a scaffold for virus assembly by interacting with both structural and nonstructural proteins. J. Virol. 85, 86–97.

MacKinnon, R., 2003. Potassium channels. FEBS Lett. 555, 62–65.

Madan, V., Sanz, M.A., Carrasco, L., 2005. Requirement of the vesicular system for membrane permeabilization by Sindbis virus. Virology 332, 307–315.

Madan, V., Sánchez-Martínez, S., Vedovato, N., Rispoli, G., Carrasco, L., Nieva, J.L., 2007. Plasma membrane-porating domain in polio virus 2B protein. A short peptide mimics viroporin activity. J. Membr. Biol. 374, 951–964.

Maldarelli, F., Chen, M.Y., Willey, R.L., Strebel, K., 1993. Human-immunodeficiency-virus type-1 Vpu protein is an oligomeric type-I integral membrane protein. J. Virol. 67, 5056–5061.

Marassi, F.M., Ma, C., Gratkowski, H., Straus, S.K., Strebel, K., Oblatt-Montal, M., et al., 1999. Correlation of the structural and functional domains in the membrane protein Vpu from HIV-1. Proc. Natl. Acad. Sci. USA 96, 14336–14341.

Margottin, F., Benichou, S., Durand, H., Richard, V., Liu, L.X., Benarous, R., 1996. Interaction between the cytoplasmic domains of HIV-1 Vpu and CD4: role of Vpu residues involved in CD4 interaction and *in vitro* CD4 degradation. Virology 223, 381–386.

Maroun, R.G., Gayet, S., Benleulmi, M.S., Porumb, H., Zargarian, L., Merad, H., et al., 2001. Peptide inhibitors of HIV-1 integrase dissociate the enzyme oligomers. Biochemistry 40, 13840–13848.

Marra, M.A., Jones, S.J.M., Astell, C.R., Holt, R.A., Brooks-Wilson, A., Butterfield, Y.S.N., et al., 2003. The genome sequence of the SARS-associated coronavirus. Science 300, 1399–1404.

Maynard, M., Pradat, P., Bailly, F., Rozier, F., Nemoz, C., Ahmed, S.N.S., et al., 2006. Amantadine triple therapy for non-responder hepatitis C patients. Clues for controversies (ANRS HC 03 BITRI). J. Hepatol. 44, 484–490.

McInerney, G.M., Smit, J.M., Liljestrom, P., Wilschut, J., 2004. Semliki forest virus produced in the absence of the 6K protein has an altered spiek structure as revealed by decreased membrane fusion capability. Virology 325, 200–206.

Mehmel, M., Rothermel, M., Meckel, T., Van Etten, J.L., Moroni, A., Thiel, G., 2003. Possible function for virus encoded K^+ channel Kcv in the replication of chlorella virus PBCV-1. FEBS Lett. 552, 7–11.

Mehnert, T., Lam, Y.H., Judge, P.J., Routh, A., Fischer, D., Watts, A., et al., 2007. Towards a mechanism of function of the viral ion channel Vpu from HIV-1. J. Biomol. Struct. Dyn. 24, 589–596.

Mehnert, T., Routh, A., Judge, P.J., Lam, Y.H., Fischer, D., Watts, A., et al., 2008. Biophysical characterisation of Vpu from HIV-1 suggests a channel-pore dualism. Proteins 70, 1488–1497.

Melton, J.V., Ewart, G.D., Weir, R.C., Board, P.G., Lee, E., Gage, P.W., 2002. Alphavirus 6K proteins form ion channels. J. Biol. Chem. 277, 46923–46931.

Miyazawa, A., Fujiyoshi, Y., Unwin, N., 2003. Structure and gating mechanism of the acetylcholine receptor pore. Nature 423, 949–955.

Montal, M., 2003. Structure-function correlates of Vpu, a membrane protein of HIV-1. FEBS Lett. 552, 47–53.

Montserret, R., Saint, N., Vanbelle, C., Salvay, A.G., Simorre, J.P., Ebel, C., et al., 2010. NMR structure and ion channel activity of the p7 protein from Hepatitis C virus. J. Biol. Chem. 285, 31446–31461.

Moore, P.B., Zhong, Q., Husslein, T., Klein, M.L., 1998. Simulation of the HIV-1 Vpu transmembrane domain as a pentameric bundle. FEBS Lett. 431, 143–148.

Mould, J.A., Li, H.C., Dudlak, C.S., Lear, J.D., Pekosz, A., Lamb, R.A., et al., 2000. Mechanism for proton conduction of the M_2 ion channel of influenza A virus. J. Biol. Chem. 275, 8592–8599.

Mould, J.A., Paterson, R.G., Takeda, M., Ohigashi, Y., Venkataraman, P., Lamb, R.A., et al., 2003. Influenza B virus BM2 protein has ion channel activity that conducts protons across membranes. Dev. Cell 5, 175–184.

Mueller, M., Grauschopf, U., Maier, T., Glockshuber, R., Ban, N., 2009. The structrure of a cytolytic alpha-helical toxin pore reveals its assembly mechanism. Nature 459, 726–730.

Myint, S.H., 1995. Human coronavirus infection. In: Siddell, S. (Ed.), The Coronaviridae. Plenum Press, New York, pp. 389–401.

Narayanan, K., Huang, C., Makino, S., 2008. SARS coronavirus accessory proteins. Virus Res. 133, 113–121.

Neil, S.J.D., Zang, T., Bieniasz, P.D., 2008. Tetherin inhibits retrovirus release and is antagonized by HIV-1 Vpu. Nature 451, 425–431.

Neupärtl, M., Meyer, C., Woll, I., Frohns, F., Kang, M., Van Etten, J.L., et al., 2008. Chlorella viruses evoke a rapid release of K+ from host cells during the early phase of infection. Virology 372, 340–348.

Neutze, R., Pebay-Peyroula, E., Edman, K., Royant, A., Navarro, J., Landau, E.M., 2002. Bacteriorhodopsin: a high-resolution structural view of vectorial proton transport. Biochim. Biophys. Acta 1565, 144–167.

Nishimura, K., Kim, S., Zhang, L., Cross, T.A., 2002. The closed state of a H^+ channel helical bundle combining precise orientational and distance restraints from solid state NMR. Biochemistry 41, 13170–13177.

Noskov, S.Y., Roux, B., 2006. Ion selectivity in potassium channels. Biophys. Chem. 124, 279–291.

Odagiri, T., Hong, J., Ohara, Y., 1999. The BM2 protein of influenza B virus is synthesized in the late phase of infection and incorporated into virions as a subviral component. J. Gen. Virol. 80, 2573–2581.

Oesterhelt, D., Stoeckenius, W., 1971. Rhodopsin-like protein from purple membrane of Halobacterium halobium. Nat. New Biol. 233, 149–152.

Park, R.R., 2000. Genetic selection for dissociative inhibitors of designated protein/protein interactions. Nat. Biotechnol. 18, 847–851.

Park, S.H., Opella, S.J., 2005. Tilt angle of a trans-membrane helix is determined by hydrophobic mismatch. J. Mol. Biol. 350, 310–318.
Park, S.H., Mrse, A.A., Nevzorov, A.A., Mesleh, M.F., Oblatt-Montal, M., Montal, M., et al., 2003. Three-dimensional structure of the channel-forming trans-membrane domain of virus protein "u" (Vpu) from HIV-1. J. Mol. Biol. 333, 409–424.
Park, S.H., Mrse, A.A., Nevzorov, A.A., De Angelis, A.A., Opella, S.J., 2006. Rotational diffusion of membrane proteins in aligned phospholipid bilayers by solid-state NMR spectroscopy. J. Magn. Reson. 178, 162–165.
Parthasarathy, K., Ng, L., Lin, X., Liu, D.-X., Pervushin, K., 2008. Structural flexibility of the pentameric SARS coronavirus envelope protein ion channel. Biophys. J. 95, L39–L41.
Patargias, G., Zitzmann, N., Dwek, R., Fischer, W.B., 2006. Protein-protein interactions: modeling the hepatitis C virus ion channel p7. J. Med. Chem. 49, 648–655.
Patargias, G., Barke, T., Watts, A., Fischer, W.B., 2009. Model generation of viral channel forming 2B protein bundles from polio and coxsackie viruses. Mol. Membr. Biol. 26, 309–320.
Patargias, G., Ewart, G., Luscombe, C., Fischer, W.B., 2010. Ligand-protein docking studies of potential HIV-1 drug compounds using the algorithm FlexX. Anal. Bioanal. Chem. 396, 2559–2563.
Paterson, R.G., Takeda, M., Ohigashi, Y., Pinto, L.H., Lamb, R.A., 2003. Influenza B virus BM2 protein is an oligomeric integral membrane protein expressed at the cell surface. Virology 306, 7–17.
Paul, M., Jabbar, M.A., 1997. Phosphorylation of both phosphoacceptor sites in the HIV-1 Vpu cytoplasmic domain is essential for Vpu-mediated ER degradation of CD4. Virology 232, 207–216.
Pavlovic, D., Neville, D.C.A., Argaud, O., Blumberg, B., Dwek, R.A., Fischer, W.B., et al., 2003. The hepatitis C virus p7 protein forms an ion channel that is inhibited by long-alkyl-chain iminosugar derivatives. Proc. Natl. Acad. Sci. USA 100, 6104–6108.
Perozo, E., Rees, D.C., 2003. Structure and mechanism in prokaryotic mechanosensitive channels. Curr. Opin. Struct. Biol. 13, 432–442.
Pervushin, K., Tan, E., Parthasarathy, K., Lin, X., Jiang, F.-L., Yu, D., et al., 2009. Structure and inhibition of the SARS Coronavirus envelope protein ion channel. PLoS Pathog. 5, e1000511.
Pielak, R.M., Chou, J.J., 2010. Flu channel drug resistance: a tale of two sides. Protein Cell 1, 246–258.
Pielak, R.M., Schnell, J.R., Chou, J.J., 2009. Mechanism of drug inhibition and drug resistance of influenza A M2 channel. Proc. Natl. Acad. Sci. USA 106, 7379–7384.
Pinto, L.H., Lamb, R.A., 1995. Understanding the mechanism of action of the anti influenza virus drug amantadine. Trends Microbiol. 3, 271.
Pinto, L.H., Dieckmann, G.R., Gandhi, C.S., Papworth, C.G., Braman, J., Shaughnessy, M. A., et al., 1997. A functionally defined model for the M2 proton channel of influenza A virus suggests a mechanism for its ion selectivity. Proc. Natl. Acad. Sci. USA 94, 11301–11306.
Plugge, B., Gazzarrini, S., Nelson, M., Cerana, R., Van Etten, J.L., Derst, C., et al., 2000. A potassium channel protein encoded by chlorella virus PBCV-1. Science 287, 1641–1644.
Poveda, E., Briz, V., Soriano, V., 2005. Enfuvirtide, the first fusion inhibitor to treat HIV infection. AIDS Rev. 7, 139–147.
Premkumar, A., Wilson, L., Ewart, G.D., Gage, P.W., 2004. Cation-selective ion channels formed by p7 of hepatitis C virus are blocked by hexamethylene amiloride. FEBS Lett. 557, 99–103.

Ramsey, I.S., Mokrab, Y., Carvacho, I., Sands, Z.A., Sansom, M.S.P., Clapham, D.E., 2010. An aqueous H^+ permeation pathway in the voltage-gated proton channel Hv1. Nat. Struct. Mol. Biol. 17, 869–875.

Rapedius, M., Fowler, P.W., Shang, L., Sansom, M.S.P., Tucker, S.J., Baukrowitz, T., 2007. H bonding at the helix-bundle crossing controls gating in Kir potassium channels. Neuron 55, 602–614.

Rishabh, P., Singh, A.V., Awanish, P., Poonam, T., Majumdar, D., Nath, L.K., 2009. Protein and peptide drugs: a brief review. Research J. Pharm. Technol. 2, 228–233.

Rödig, C., Chizhov, I., Weidlich, O., Siebert, F., 1999. Time-resolved step-scan Fourier transform infrared spectroscopy reveals differences between early and late M intermediates of bacteriorhodopsin. Biophys. J. 76, 2687–2701.

Römer, W., Lam, Y.H., Fischer, D., Watts, A., Fischer, W.B., Göring, P., et al., 2004. Channel activity of a viral transmembrane peptide in micro-BLMs: Vpu_{1-32} from HIV-1. J. Am. Chem. Soc. 126, 16267–16274.

Root, M.J., Kay, M.S., Kim, P.S., 2001. Protein design of an HIV-1 entry inhibitor. Science 291, 884–888.

Rothschild, K.J., 1992. FTIR difference spectroscopy of bacteriorhodopsin: towards a molecular model. J. Bioenerg. Biomembr. 24, 147–167.

Rouse, S.L., Carpenter, T., Stansfield, P.J., Sansom, M.S.P., 2009. Simulations of the BM2 proton channel transmembrane domain from influenza virus B. Biochemistry 48, 9949–9951.

Ruiz, A., Hill, M.S., Schmitt, K., Guatelli, J., Stephens, E.B., 2008. Requirements of the membrane proximal tyrosine and dileucine-based sorting signals for effective transport of the subtype C Vpu protein to the plasma membrane and virus release. Virology 378, 58–68.

Ruiz, A., Guatelli, J., Stephens, E.B., 2010a. The Vpu protein: new concepts in virus release and CD4 down-modulation. Curr. HIV Res. 8, 240–252.

Ruiz, A., Hill, M.S., Schmitt, K., Stephens, E.B., 2010b. Membrane raft association of the Vpu protein of human immunodeficiency virus type 1 correlates with enhanced virus release. Virology 408, 89–102.

Saint, N., Lacapére, J.-J., Gu, L.Q., Ghazi, A., Martinac, B., Rigaud, J.-L., 1998. A hexameric transmembrane pore revealed by two-dimensional crystallization of the large mechanosensitive ion channel (MscL) of *Escherichia coli*. J. Biol. Chem. 273, 14667–14670.

Sansom, M.S.P., Kerr, I.D., 1993. Influenza virus M_2 protein: a molecular modelling study on the ion channel. Protein Eng. 6, 65–74.

Sansom, M.S., Kerr, I.D., Smith, G.R., Son, H.S., 1997. The influenza A virus M2 channel: a molecular modelling and simulation study. Virology 233, 163–173.

Sansom, M.S.P., Shrivastava, I.H., Bright, J.N., Tate, J., Capener, C.E., Biggin, P.C., 2002. Potassium channels: structures, models, simulations. Biochim. Biophys. Acta 1565, 294–307.

Sanz, M.A., Madan, V., Carrasco, L., Nieva, J.L., 2003. Interfacial domains in Sindbis virus 6K protein. J. Biol. Chem. 278, 2051–2057.

Schindler, C., Fischer, W.B., 2011. Sequence alignment of viral channel proteins with cellular ion channels and toxins. in preparation.

Schlesinger, S.S., Schlesinger, M.J., 1986. Formation and assembly of alphavirus glycoproteins. In: Schlesinger, S.S., Schlesinger, M.J. (Eds.), The Togaviridae and Flaviviridae. Plenum Press, New York, pp. 121–148.

Schmitt, U.W., Voth, G.A., 1998. Multistate empirical valence bond model for proton transport in water. J. Phys. Chem. B 102, 5547–5551.

Schnell, J.R., Chou, J.J., 2008. Structure and mechanism of the M2 proton channel of influenza A virus. Nature 451, 591–595.

Schroeder, C., 2010. Cholesterol-binding viral proteins in virus entry and morphogenesis. Subcell. Biochem. 51, 77–108.

Schroeder, C., Lin, T.-I., 2005. Influenza A virus M2 protein: proton selectivity of the ion channel, cytotoxicity, and a hypothesis on peripheral raft association and virus budding. In: Fischer, W.B. (Ed.), Viral Membrane Proteins: Structure, Function, and Drug Design. Kluwer Academic, New York, pp. 113–130.

Schroeder, C., Ford, C.M., Wharton, S.A., Hay, A.J., 1994. Functional reconstitution in lipid vesicles of influenza virus M2 protein expressed by baculovirus: evidence for proton transfer activity. J. Gen. Virol. 75, 3477–3484.

Schroeder, C., Heider, H., Moncke-Buchner, E., Lin, T.I., 2005. The influenza virus ion channel and maturation cofactor M2 is a cholesterol-binding protein. Eur. Biophys. J. 34, 52–66.

Schubert, U., Henklein, P., Boldyreff, B., Wingender, E., Strebel, K., Porstmann, T., 1994. The human immunodeficiency virus type 1 encoded Vpu protein is phosphorylated by casein kinase-2 (CK-2) at positions Ser52 and Ser54 within a predicted alpha-helix-turn-alpha-helix-motif. J. Mol. Biol. 236, 16–25.

Schubert, U., Bour, S., Ferrer-Montiel, A.V., Montal, M., Maldarelli, F., Strebel, K., 1996a. The two biological activities of human immunodeficiency virus type 1 Vpu protein involve two separable structural domains. J. Virol. 70, 809–819.

Schubert, U., Ferrer-Montiel, A.V., Oblatt-Montal, M., Henklein, P., Strebel, K., Montal, M., 1996b. Identification of an ion channel activity of the Vpu transmembrane domain and its involvement in the regulation of virus release from HIV-1-infected cells. FEBS Lett. 398, 12–18.

Schubert, H.L., Zhai, Q., Sandrin, V., Eckert, D.M., Garcia-Maya, M., Saul, L., et al., 2010. Structural and functional studies on the extracellular domain of BST2/tetherin in reduced and oxidized conformations. Proc. Natl. Acad. Sci. USA 107, 17951–17956.

Schwarz, S., Wang, K., Yu, W., Sun, B., Schwarz, W., 2011. Emodin inhibits current through SARS-associated coronavirus 3a protein. Antiviral Res. 90, 64–69.

Schweighofer, K.J., Pohorille, A., 2000. Computer simulation of ion channel gating: The M_2 channel of influenza A virus in a lipid bilayer. Biophys. J. 78, 150–163.

Scott, R.W., DeGrado, W.F., Tew, G.N., 2008. De novo designed synthetic mimics of antimicrobial peptides. Curr. Opin. Biotechnol. 19, 620–627.

Shai, Y., Oren, Z., 2001. From 'carpet' mechanism to de-novo designed diastereomeric cell-selective antimicrobial peptides. Peptides 22, 1629–1641.

Shaji, J., Patole, V., 2008. Protein and peptide drug delivery: oral approaches. Indian J. Pharm. Sci. 70, 269–277.

Sharma, M., Yi, M., Dong, H., Qin, H., Peterson, E., Busath, D.D., et al., 2010. Insight into the mechanism of the influenza A proton channel from a structure in a lipid bilayer. Science 330, 509–512.

Sharpe, S., Yau, W.M., Tycko, R., 2006. Structure and dynamics of the HIV-1 Vpu transmembrane domain revealed by solid-state NMR with magic-angle spinning. Biochemistry 45, 918–933.

Shen, X., Xue, J.H., Yu, C.Y., Luo, H.B., Qin, L., Yu, X.J., et al., 2003. Small envelope protein E of SARS: cloning, expression, purification, CD determination, and bioinformatics analysis. Acta Pharmacol. Sin. 24, 505–511.

Shimbo, K., Brassard, D.L., Lamb, R.A., Pinto, L.H., 1996. Ion selectivity and activation of the M_2 ion channel of Influenza virus. Biophys. J. 70, 1335–1346.

Simons, K., Ikonen, E., 1997. Functional rafts in cell membranes. Nature 387, 569–572.

Skasko, M., Tokarev, A., Chen, C.-C., Fischer, W.B., Pillai, S.K., Guatelli, J., 2011. BST-2 is rapidly down-regulated from the cell surface by the HIV-1 protein Vpu: evidence for a post-ER mechanism of Vpu-action. Virology 411, 65–77.

Smondyrev, A.M., Voth, G.A., 2002. Molecular dynamics simulation of proton transport through the influenza A virus M2 channel. Biophys. J. 83, 1987–1996.

Song, L., Hobaugh, M.R., Shustak, C., Cheley, S., Bayley, H., Gouaux, J.E., 1996. Structure of staphylococcal alpha-hemolysin, a heptameric transmembrane pore. Science 274, 1859–1866.

Sonnhammer, E.L., von Heijne, G., Krogh, A., 1998. A hidden Markov model for predicting transmembrane helices in protein sequences. Proc. Int. Conf. Intell. Syst. Mol. Biol. 6, 175–182.

Sramala, I., Lemaitre, V., Faraldo-Gomez, J.D., Vincent, S., Watts, A., Fischer, W.B., 2003. Molecular dynamics simulations on the first two helices of Vpu from HIV-1. Biophys. J. 84, 3276–3284.

Stadler, K., Masignani, V., Eickmann, M., Becker, S., Abrignani, S., Klenk, H.-D., et al., 2003. SARS—beginning to understand a new virus. Nat. Rev. Microbiol. 1, 209–218.

Steffen, I., Pöhlmann, S., 2010. Peptide-based inhibitors of the HIV envelope protein and other class I viral fusion proteins. Curr. Pharm. Des. 16, 1143–1158.

Steinbacher, S., Bass, R., Strop, P., Rees, D.C., 2007. Structures of the prokaryotic mechanosensitive channels MscL and MscS. Curr. Top. Membr. 58, 1–24.

Steinmann, E., Penin, F., Kallis, S., Patel, A.H., Bartenschlager, R., Pietschmann, T., 2007a. Hepatitis C virus p7 protein is crucial for assembly and release of infectious virions. PLoS Pathog. 3, 962–971.

Steinmann, E., Whitfield, T., Kallis, S., Dwek, R., Zitzmann, N., Pietschmann, T., et al., 2007b. Antiviral effects of amantadine and iminosugar derivatives against hepatitis C virus. Hepatology 46, 330–338.

Stier, A., Sackmann, E., 1973. Spin labels as enzyme substrates. Heterogeneous lipid distribution in liver microsomal membranes. Biochim. Biophys. Acta 311, 400–408.

Stouffer, A.L., Acharya, R., Salom, D., Levine, A.S., Di Constanzo, L., Soto, C.S., et al., 2008. Structural basis for the function and inhibition of an influenza virus proton channel. Nature 451, 596–599.

Strangler, T., Tran, T., Hoffmann, S., Schmidt, H., Jonas, E., Willbold, D., 2007. Competitive displacement of full-length HIV-1 Nef from the Hck SH3 domain by a high-affinity artificial peptide. Biol. Chem. 388, 611–615.

Strauss, J.H., Strauss, E.G., 1994. The Alphaviruses: gene expression, replication, and evolution. Microbiol. Rev. 58, 491–562.

Strebel, K., Klimkait, T., Martin, M.A., 1988. Novel gene of HIV-1, *vpu*, and its 16-kilodalton product. Science 241, 1221–1223.

Strebel, K., Klimkait, T., Maldarelli, F., Martin, M.A., 1989. Molecular and biochemical analysis of human deficiency virus type 1 *vpu* protein. J. Virol. 63, 3784–3791.

Strockbine, B., Rizzo, R.C., 2007. Binding of antifusion peptides with HIVgp41 from molecular dynamics simulations: quantitative correlation with experiments. Proteins 67, 630–642.

Sugrue, R.J., Hay, A.J., 1991. Structural characteristics of the M2 protein of influenza A viruses: evidence that it forms a tetrameric channel. Virology 180, 617–624.

Sugrue, R.J., Belshe, R.B., Hay, A.J., 1990. Palmitoylation of the influenza A virus M_2 protein. Virology 179, 51–56.

Sukharev, S.I., Schroeder, M.J., McCaslin, D.R., 1999. Stoichiometry of the large conductance bacterial mechanosensitive channel of E. coli. A biochemical study. J. Membr. Biol. 171, 183–193.

Sun, F., 2003. Molecular dynamics simulation of human immunodificiencey virus protein U (Vpu) in lipid/water Lamgmuir monolayer. J. Mol. Model. 9, 114–123.

Tan, Y.-J., Teng, E., Shen, S., Tan, T.H.P., Goh, P.-Y., Fielding, B.C., et al., 2004. A novel severe acute respiratory syndrome coronavirus protein, U274, is transported to the cell surface and undergoes endocytosis. J. Virol. 78, 6723–6734.

Tayefeh, S., Kloss, T., Thiel, G., Hertel, B., Moroni, A., Kast, S.M., 2007. Molecular dynamics simulation study of the cytosolic mouth in Kcv-type potassium channels. Biochemistry 46, 4826–4839.

Tayefeh, S., Kloss, T., Kreim, M., Gebhardt, M., Baumeister, D., Hertel, B., et al., 2009. Model development for the viral Kcv potassium channel. Biophys. J. 96, 485–498.

Tedbury, P., Welbourn, S., Pause, A., King, B., Griffin, S., Harris, M., 2011. The sub-cellular localisation of the hepatitis C virus non-structural protein NS2 is regulated by an ion channel-independent function of the p7 protein. J. Gen. Virol. 92, 819–830.

Terwilliger, E.F., Cohen, E.A., Lu, Y., Sodroski, J.G., Haseltine, W.A., 1989. Functional role of human immunodeficiency virus type 1 vpu. Proc. Natl. Acad. Sci. USA 86, 5163–5167.

Tian, C., Tobler, K., Lamb, R.A., Pinto, L.H., Cross, T.A., 2002. Expression and initial structural insights from solid-state NMR of the M2 proton channel from influenza A virus. Biochemistry 41, 11294–11300.

Tian, C., Gao, P.F., Pinto, L.H., Lamb, R.A., Cross, T.A., 2003. Initial structural and dynamic characterization of the M2 protein transmembrane and amphipathic helices in lipid bilayers. Protein Sci. 12, 2597–2605.

Tiganos, E., Yao, X.-J., Friborg, J., Daniel, N., Cohen, E.A., 1997. Putative a-helical structures in the Human immunodeficiency virus type 1 Vpu protein and CD4 are involved in binding and degradation of the CD4 molecule. J. Virol. 71, 4452–4460.

Tiganos, E., Friborg, J., Allain, B., Daniel, N.G., Yao, X.-J., Cohen, E.A., 1998. Structural and functional analyis of the membrane-spanning domain of the Human Immunodeficiency Virus Type 1 Vpu protein. Virology 251, 96–107.

Tosteson, M.T., Pinto, L.H., Holsinger, L.J., Lamb, R.A., 1994. Reconstitution of the Influenza virus M_2 ion channel in lipid bilayers. J. Membr. Biol. 142, 117–126.

Unwin, N., 1995. Acetylcholine receptor channel imaged in the open state. Nature 373, 37–43.

Unwin, N., 1998. The nicotinic acetylcholine receptor of *Torpedo* electric ray. J. Struc. Biol. 121, 181–190.

Unwin, N., 2003. Structure and action of the nicotinic acetylcholine receptor explored by electron microscopy. FEBS Lett. 555, 91–95.

Unwin, N., 2005. Refined structure of the nicotinic acetylcholine receptor at 4 Å resolution. J. Mol. Biol. 346, 967–989.

Unwin, N., Toyoshima, C., Kubalek, E., 1988. Arrangement of the acetylcholine receptor subunits in the resting and desensitized states, determined by cryoelectron microscopy of crystallized Torpedo postsynaptic membranes. J. Cell Biol. 107, 1123–1138.

van Damme, N., Goff, D., Katsura, C., Jorgensen, R.L., Mitchell, R., Johnson, M.C., et al., 2008. The interferon-induced protein BST-2 restricts HIV-1 release and is downregulated from the cell surface by the viral Vpu protein. Cell Host Microbe 3, 1–8.

van Kuppeveld, F.J., Galama, J.M., Zoll, J., Melchers, W.J., 1995. Genetic analysis of a hydrophobic domain of coxsackie B3 virus protein 2B: a moderate degree of hydrophobicity is required for a cis-acting function in viral RNA synthesis. J. Virol. 69, 7782–7790.

van Kuppeveld, F.J.M., Hoenderop, J.G.J., Smeets, R.L.L., Willems, P.H.G.M., Dijkman, H.B.P.M., Galama, J.M.D., et al., 1997a. Coxsackievirus protein 2B modifies endoplasmic reticulum membrane and plasma membrane permeability and facilitates virus release. EMBO J. 16, 3519–3532.

van Kuppeveld, F.J.M., Melchers, W.J.G., Kirkegaard, K., Doedens, J.R., 1997b. Structure-function analysis of coxsackie B3 virus protein 2B. Virology 227, 111–118.

van Kuppeveld, F.J.M., Melchers, W.J.G., Willems, P.H.G.M., Gadella Jr., T.W.J., 2002. Homomultimerization of the coxsackievirus 2B protein in living cells visualized by fluorescence resonance energy transfer microscopy. J. Virol. 76, 9446–9456.

Verma, S.P., 2009. HIV: a raft-targeting approach for prevention and therapy using plant-derived compounds. Curr. Drug Targets 10, 51–59.

Vijayvergiya, V., Wilson, R., Chorak, A., Gao, P.F., Cross, T.A., Busath, D.D., 2004. Proton conductance of influenza virus M2 protein in planar lipid bilayers. Biophys. J. 87, 1697–1704.

Waheed, A.A., Ablan, S.D., Mankowski, M.K., Cummins, J.E., Ptak, R.G., Schaffner, C.P., et al., 2006. Inhibition of HIV-1 replication by amphotericin B methyl ester: selection for resistant variants. J. Biol. Chem. 281, 28699–28711.

Waheed, A.A., Ablan, S.D., Soheilian, F., Nagashima, K., Ono, A., Schaffner, C.P., et al., 2008. Inhibition of human immunodeficiency virus type 1 assembly and release by cholesterol-binding compound amphotericin B methyl ester: evidence for Vpu dependence. J. Virol. 82, 9776–9781.

Wang, C., Takeuchi, K., Pinto, L.H., Lamb, R.A., 1993. Ion channel activity of influenza A virus M_2 protein: characterization of the amantadine block. J. Virol. 67, 5585–5594.

Wang, C., Lamb, R.A., Pinto, L.H., 1994. Direct measurement of the Influenza A virus M_2 protein ion channel activity in mammalian cells. Virology 205, 133–140.

Wang, C., Lamb, R.A., Pinto, L.H., 1995. Activation of the M_2 ion channel of influenza virus: a role for the transmembrane domain histidine residue. Biophys. J. 69, 1363–1371.

Wang, W., Black, S.S., Edwards, M.D., Miller, S., Morrison, E.L., Bartlett, W., et al., 2008. The structure of an open form of an E. coli mechanosensitive channel at 3.45 Å resolution. Science 321, 1179–1183.

Wang, J., Cady, S.D., Balannik, V., Pinto, L.H., DeGrado, W.F., Hong, M., 2009a. Discovery of spiro-piperidine inhibitors and their modulation of the dynamics of the M2 proton channel from influenza A virus. J. Am. Chem. Soc. 131, 8066–8076.

Wang, J., Pielak, R.M., McClintock, M.A., Chou, J.J., 2009b. Solution structure and functional analysis of the influenza B proton channel. Nat. Struct. Biol. 16, 1267–1271.

Wang, K., Xie, S., Sun, B., 2010a. Viral proteins function as ion channels. Biochim. Biophys. Acta 1808, 510–515.

Wang, Y., Xu, H., Wu, N., Shi, H., Wang, X., Wang, T., 2010b. Monoclonal antibody, but not synthetic peptide, targeting the ectodomain of influenza B virus M2 proton channel has antiviral activity. New Microbiol. 33, 311–317.

Wang, J., Qiu, J.X., Soto, C., DeGrado, W.F., 2011. Structural and dynamic mechanisms for the function and inhibition of the M2 proton channel from influenza A virus. Curr. Opin. Struct. Biol. 21, 68–80.

Watt, P.M., Heinrich, T.K., Thomas, W.R., 2006. Protein silencing with Phylomers: a new tool for target validation and generating lead biologicals targeting protein interactions. Expert Opin. Drug Discov. 1, 491–502.

Welch, B.D., VanDenmark, A.P., Heroux, A., Hill, C.P., Kay, M.S., 2007. Potent D-peptide inhibitors of HIV-1 entry. Proc. Natl. Acad. Sci. USA 104, 16828–16833.

Whitfield, T., Miles, A.J., Scheinost, J.C., Offer, J., Wentworth Jr., P., Dwek, R.A., et al., 2011. The influence of different lipid environment on the structure and function of the hepatitis C virus p7 ion channel protein. Mol. Membr. Biol. 28, 254–264.

Willbold, D., Hoffmann, S., Rösch, P., 1997. Secondary structure and tertiary fold of the human immunodeficiency virus protein U (Vpu) cytoplasmatic domain in solution. Eur. J. Biochem. 245, 581–588.

Willey, R.L., Maldarelli, F., Martin, M.A., Strebel, K., 1992a. Human immunodeficiency virus type 1 Vpu protein induces rapid degradation of CD4. J. Virol. 66, 7193–7200.

Willey, R.L., Maldarelli, F., Martin, M.A., Strebel, K., 1992b. Human immunodeficiency virus type 1 Vpu protein regulates the formation of intracellular gp160-CD4 complexes. J. Virol. 66, 226–234.

Wilson, L., McKinlay, C., Gage, P., Ewart, G., 2004. SARS coronavirus E protein forms cation-selective ion channels. Virology 330, 322–331.

Wink, M., 2008. Evolutionary advantage and molecular modes of action of multi-component mixtures used in phytomedicine. Curr. Drug Metab. 9, 996–1009.

Winter, G., Fields, S., 1980. Cloning of influenza cDNA into M13: the sequence of the RNA segment encoding the A/PR/8/34 matrix protein. Nucleic Acids Res. 8, 1965–1974.

Winter, R., Nozirov, F., Sternberg, U., Cross, T.A., Ulrich, A.S., Fu, R., 2008. Solid-state 19F NMR spectroscopy reveals that Trp41 participates in the gating mechanism of the M2 proton channel of influenza A virus. J. Am. Chem. Soc. 130, 918–924.

Wittlich, M., Koenig, B.W., Willbold, D., 2008. Structural consequences of phosphorylation of two serine residues in the cytiplasmic domain of HIV-1 VpU. J. Pept. Sci. 14, 804–810.

Wittlich, M., Koenig, B.W., Stoldt, M., Schmidt, H., Willbold, D., 2009. NMR structural characterization of HIV-1 virus protein U cytoplasmic domain in the presence of dodecylphosphatidylcholine micelles. FEBS J. 276, 6560–6575.

Wray, V., Federau, T., Henklein, P., Klabunde, S., Kunert, O., Schomburg, D., et al., 1995. Solution structure of the hydrophilic region of HIV-1 encoded virus protein U (Vpu) by CD and ^{1}H NMR-spectroscopy. Int. J. Pept. Protein Res. 45, 35–43.

Wray, V., Kinder, R., Federau, T., Henklein, P., Bechinger, B., Schubert, U., 1999. Solution structure and orientation of the transmembrane anchor domain of the HIV-1 -encoded virus protein U by high resolution and solid-state NMR spectroscopy. Biochemistry 38, 5272–5282.

Xie, S., Wang, K., Yu, W., Lu, W., Xu, K., Wang, J., et al., 2011. 2B protein of enterovirus 71 induces chloride-dependent current and can be blocked by DIDS. Cell Res. 21, 1271–1275.

Yamada, T., Onimatsu, H., van Etten, J.L., 2006. Chlorella viruses. Adv. Virus Res. 66, 293–336.

Yi, M., Cross, T.A., Zhou, H.-X., 2008. A secondary gate as a mechanism for inhibition of the M2 proton channel by amantadine. J. Phys. Chem. B 112, 7977–7979.

Yu, C.J., Chen, Y.C., Hsiao, C.H., Kuo, T.C., Chang, S.C., Lu, C.Y., et al., 2004. Identification of a novel protein 3a from severe acute respiratory syndrome coronavirus. FEBS Lett. 565, 111–116.

Yuan, X., Li, J., Shan, Y., Yang, Z., Zhao, Z., Chen, B., et al., 2005. Subcellular localization and membrane association of SARS-CoV 3a protein. Virus Res. 109, 191–202.

Zebedee, S.L., Lamb, R.A., 1988. Influenza A virus M_2 protein: Monoclonal antibody restriction of virus growth and detection of M_2 in virions. J. Virol. 62, 2762–2772.

Zeng, R., Yang, R.-F., Shi, M.-D., Jiang, M.-R., Xie, Y.-H., Ruan, H.-Q., et al., 2004. Characterization of the 3a protein of SARS-associated coronavirus in infected Vero E6 cells and SARS patients. J. Mol. Biol. 341, 271–279.

Zhao, L., O'Reilly, M.K., Shultz, M.D., Chmielewski, J., 2003. Interfacial peptide inhibitors of HIV-1 integrase activity and dimerization. Bioorg. Med. Chem. Lett. 13, 1175–1177.

Zheng, S., Strzalka, J., Ma, C., Opella, S.J., Ocko, B.M., Blasie, J.K., 2001. Structural studies of the HIV-1 accessory protein Vpu in Langmuir monolayers: synchroton X-ray reflectivity. Biophys. J. 80, 1837–1850.

Zhong, Q., Husslein, T., Moore, P.B., Newns, D.M., Pattnaik, P., Klein, M.L., 1998. The M2 channel of influenza A virus: a molecular dynamics study. FEBS Lett. 434, 265–271.

Zhong, N.S., Zheng, B.J., Li, Y.M., Poon, L.L.M., Xie, Z.H., Chan, K.H., et al., 2003. Epidemiology and cause of severe acute respiratory syndrom (SARS) in Guangdong, People's Republic of China, February, 2003. Lancet 362, 1353–1358.

Zhou, X.-L., Stumpf, M.A., Hoch, H.C., Kung, C., 1991. A mechanosensitive channel in whole cells and in membrane patches of the fungus *Uromyces*. Science 253, 1415–1417.